

Master thesis:

Age Estimates and Distribution of the Black dogfish (*Centroscyllium fabricii*)



Student

Trine Qvist, 201206141

Supervisors

Peter Grønkjær, Aarhus University

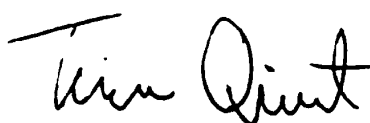
Rasmus Hedeholm, Greenland Institute of Natural Resources

Julius Nielsen, University of Copenhagen

November 2017

Preface

This Master's thesis is a 60 ECTS experimental science project made in collaboration with Aarhus University and the Greenland Institute of Natural Resources (GIRN) and conducted during the period February to November 2017. The project is funded by the Greenland Research Council and aims to estimate the age of the black dogfish (*Centroscyllium fabricii*) and moreover to describe its distribution around Greenland. Data was collected by GIRN from both East and West Greenland during the period June to September 2016. Field work was conducted in October 2016 at GIRN in Nuuk, Greenland. Supplementary catch data containing yearly bottom trawl surveys in Greenland waters conducted by GIRN since 1991 was also provided for this project. Supervision and support was provided by the main supervisor Peter Grønkjær, Department of Bioscience – Aquatic Biology, Aarhus University, and the project supervisors Rasmus B. Hedeholm, Department of fish and shellfish, GIRN and Julius Nielsen, Department of Bioscience – Marine Biology, University of Copenhagen. The work has been carried out at GIRN, at the Department of Bioscience (Aarhus University) and at the Department of Physics and Astronomy (Aarhus University).



Trine Qvist, student number 201206141
Bioscience, Aarhus University, Denmark
Submission date: 20.11.2017

Table of content

| | |
|---|-----------|
| PREFACE | 1 |
| ACKNOWLEDGMENT | 3 |
| ABSTRACT | 4 |
| RESUMÉ | 5 |
| 1 INTRODUCTION | 6 |
| 1.1 THE BLACK DOGFISH | 6 |
| 1.2 DISTRIBUTION | 7 |
| 1.3 LIFE HISTORY CHARACTERISTICS | 8 |
| 1.3.1 Growth pattern | 8 |
| 1.3.2 Age and size at maturity | 9 |
| 1.3.3 Longevity and natural mortality | 9 |
| 1.4 ESTIMATION AND VALIDATION OF AGE IN ELASMOBRANCHS | 10 |
| 1.4.1 The dorsal fin spines | 11 |
| 1.4.2 Radiocarbon dating | 12 |
| 1.4.3 The eye lens | 14 |
| 1.5 MATURITY AND REPRODUCTION | 15 |
| 2 MATERIAL AND METHODS | 16 |
| 2.1 SAMPLING, SURVEY | 16 |
| 2.2 SAMPLING & BIOLOGICAL ANALYSIS | 17 |
| 2.3 AGE ESTIMATION | 18 |
| 2.3.1 Fin spine preparation | 18 |
| 2.3.2 External bands | 18 |
| 2.3.3 Cross-sections | 19 |
| 2.4 RADIOCARBON ANALYSIS | 20 |
| 2.4.1 Eye lens preparation | 20 |
| 2.4.2 Stable isotope analysis | 20 |
| 2.5 DISTRIBUTION | 21 |
| 2.5.1 Biological information | 21 |
| 3 RESULTS | 22 |
| 3.1 AGE ESTIMATION | 22 |
| 3.1.1 External bands | 22 |
| 3.1.2 Cross-sections | 22 |
| 3.2 RADIOCARBON ANALYSIS | 28 |
| 3.3 DISTRIBUTION | 30 |
| 3.3.1 Biological information | 33 |
| 3.4 MATURITY | 35 |
| 4 DISCUSSION | 36 |
| 4.1 AGE ESTIMATION AND VALIDATION | 36 |
| 4.3 DISTRIBUTION | 40 |
| 5 CONCLUSION | 41 |
| REFERENCES | 42 |
| APPENDIX I | 47 |

Acknowledgment

First of all, I would like to thank the people at my office and at the department for creating a fun and supportive work-environment. Thanks to my main supervisor Peter Grønkjær for giving me the opportunity to carry out this interesting project and to the Greenland Research Council for making this project possible. A special thanks to my supervisors Rasmus B. Hedeholm and Julius Nielsen, for the establishment of the project, for challenging me through discussions and always taking the time to answering my many questions. Thanks to GIRN for providing both office and laboratory facilities under my stay in Nuuk. Also a special thanks to Ming-Tsung Chung and Charlotte Sirot for agreeing to be my co-readers, I could not have done it without you. Thanks to Rune Kristiansen from the Kattegat center and to the Department of Physics and Astronomy, for technical support. I am thankful for the many comments from and discussions with especially Maria Rosenlund and Luna K. Marcussen for their help proofreading the entire thesis.

Abstract

The black dogfish, *Centroscyllium fabricii* (Reinhardt, 1825) is a deep water shark, abundant throughout Greenland waters. This species is a commonly occurring by-catch species in commercial fisheries targeting the northern shrimp (*Pandalus borealis*) and juvenile stages of Greenland halibut (*Reinhardtius hippoglossoides*). However, only little is known about its biology and life strategies.

Fundamental biological questions concerning the black dogfish in Greenland waters is addressed in this study. This includes estimation of age, description of the overall distribution in Greenland and determination of age and size at maturity. In addition to historical catch data, 424 black dogfish are caught in offshore waters of Greenland between June and September 2016. Dorsal fin spines are sampled for age estimation, while eye globes are analyzed for age validation throughout measurements of ^{14}C , ^{13}C , ^{15}N and maturity stages are investigated to determine the age and size at maturity.

Using fin spine growth bands, I have provided the first age estimates for black dogfish. Based on radiocarbon dating, these estimates are however minimum estimates as the largest individuals appear to be more than 50 years old. The reason for this underestimation is unknown, but continued spine growth with length suggest it is linked with vanishingly-narrow growth bands in the layers of the fin spine or non-annual growth band deposition at older ages. Additional studies using more lengths for radiocarbon dating could shed further light on the accuracy of the age readings as could tagging studies. The data on trawl catches clearly show the distributional limit of black dogfish in both East and West Greenland. These are well connected with the dominating current system around Greenland and the temperature preferences of black dogfish. Moreover, the depth preferences are clearly shown and illustrate that the black dogfish is vulnerable as a bycatch species in bottom trawl fisheries; especially those targeting Greenland halibut.

Resumé

Sorthajen, *Centroscyllium fabricii* (Reinhard, 1825) er en dybhavshaj med stor udbredelse i det Grønlandske farvand. Den er en almindelig forekommende bifangst art i kommercielt fiskeri rettet mod dybvandsrejer (*Pandalus borealis*) og juvenile stadier af hellefisk (*Reinhardtius hippoglossoides*). Desværre ved man kun lidt om dens biologi og livsstrategier.

Fundamentale biologiske aspekter for sorthajen i Grønlandsk farvand er belyst i dette studie. Studiet omfatter alders estimering, beskrivelse af den overordnede fordeling i Grønland og bestemmelse af alder og størrelse ved modenhed. Historiske fangstdata er suppleret med data fra 424 sorthajer fanget mellem juni og september 2016. Rygpigge er indsamlet til alders estimeringer, mens øjne er analyseret som validerings metode for alder gennem målinger af ^{14}C , ^{13}C , ^{15}N og modenheds-stadier er undersøgt for at kunne bestemme alder og størrelse ved modenhed.

Ved at benytte vækst bånd fra rygpigge har jeg fremstillet de første alders estimeringer for sorthajer. Baseret på radiokarbondatering er disse resultater dog minimale estimater, da de største individer synes at være mere end 50 år gamle. Årsagen til denne underestimering er ukendt, men forsat vækst af rygpiggens længde kan skyldes forsvindende smalle vækstbånd i lagene i rygpiggene eller at aflejringen af vækstbånd ikke sker årligt. Yderligere undersøgelser kan give mere klarhed omkring nøjagtigheden af alderslæsningerne ved at bruge flere længder til radioaktivt stofdatering, det samme kan mærkningsstudier.

Oplysninger om trawlfangsterne viser tydeligt en tydelig grænse for fordelingen af sorthajer i både Øst- og Vestgrønland, hvilket er i overensstemmelse med de dominerende havstrømme omkring Grønland og temperature præferencer for sorthajen. Dybdepræferencer er også tydeligt vist og illustrere at sorthajen er sårbar som bifangst i bundtrawlfiskeri; især dem rettet mod Grønlandske hellefisk.

1 Introduction

1.1 The Black dogfish

Black dogfish, *Centroscyllium fabricii* was first described by Johannes Reinhard in 1825 and named *Spinax fabricii* (Reinhard, 1825). Later, in 1839 the new genus *Centroscyllium* was described (Compagno, 1984). Now the genus comprises six species besides the black dogfish, including the granular dogfish (*C. granulatum*), ornate dogfish (*C. ornatum*), combtooth dogfish (*C. nigrum*), highfin dogfish (*C. excelsum*), whitefin dogfish (*C. ritteri*) and bareskin dogfish (*C. kamoharai*) (Menni et al., 1990). Menni et al. (1990) explained that black dogfish in several studies was reported wrongly as what is now believed to be the granular dogfish originally described by Gunther (1887). Errors like this would have an implication for the understanding of the biology and distribution of a species, but do also testify that these sharks are considerably alike and probably difficult to distinguish between.

Black dogfish are relatively small deep-water squalid sharks. The maximum size is believed to be 107 cm (Compagno, 1984; IUCN, 2009). Black dogfish have big, reflective green eyes, a blackish-brown color, no anal fin and two dorsal fin spines, the posterior being larger than the anterior (Figure 1, Compagno, 1984; Jakobsdóttir, 2001; IUCN, 2009). Luminescent organs are scattered in the skin of the dogfish, especially on the nose, but not arranged in order, as reported in other species (Compagno, 1984). Black dogfish use bioluminescence for effective camouflage (i.e. counter-illumination) mimicking the residual downwelling light which blurs out the shadow of the shark, making hunting easier (Young, 1983; Claes et al., 2014).



Figure 1 Illustration of a black dogfish, *Centroscyllium fabricii*, (Photo credit: [Shark Trust](#)).

Unlike the spiny dogfish (*Squalus acanthias*), which have been caught and exploited for their oil since the 1870's (McFarlane and Beamish, 1987), there are no known surveys targeting black dogfish (at least not in Canada, Kulka 2006, or in Greenland). Nor is black dogfish considered in any international groups and is categorized as 'Least Concern' on the IUCN Red List (IUCN, 2009), why any population changes might go unnoticed. Little is known about its biology and life strategies, as research priorities usually are linked to an economic value of a fishery (Kulka, 2006). Black dogfish is a commonly

occurring by-catch species in commercial fisheries targeting other deep-water species such as northern shrimp (*Pandalus borealis*) or juvenile stages of Greenland halibut (*Reinhardtius hippoglossoides*) (Jakobsdóttir 2001; Jorgensen et al., 2014).

The black dogfish is an opportunistic feeder with the most important prey items being teleost, crustaceans and cephalopods (Jakobsdóttir, 2001; Qvist, unpublished data). Evidence suggest that black dogfish is an abundant and schooling shark with deep-pelagic foraging on prey in the water column (Compagno, 1984). A scavenging behavior, has been observed by finds of only heads of semi-digested redfish (*Sebastes spp.*), a fish too big for black dogfish to consume (Qvist, unpublished data). Nothing imply that black dogfish predate on key commercial species such as the northern shrimp or juvenile stages of Greenland halibut, even though they are abundant in the same area (Qvist, unpublished data), suggesting no impact on the harvestable biomass.

1.2 Distribution

A widespread but also sporadic distribution in the Atlantic Ocean has been reported for black dogfish (Kulka, 2006; IUCN, 2009). The distribution range from southern Greenland and the Baffin Island along Canada to the Gulf of Mexico, in the waters Northwest of the Atlantic Ocean (Compagno, 1984; Kulka 2006). It has also been recorded in the Northeast of the Atlantic Ocean from Iceland to the continental slope of central Africa, (Kulka 2006), but also in the deeper waters of southern Africa (>500m, IUNC 2009). According to Jakobsdóttir (2001) it is the most common deep-water dogfish in Icelandic waters, especially in areas west of Iceland. Moreover, a study by Kulka (2006) reports that it is distributed along the entire length of Canadian continental slope waters.

While black dogfish live along the edges of the Arctic Ocean, they do not seem to extend to it (Compagno, 1984; Yano 1995). Even though black dogfish are adapted to low temperatures and are reported to survive water temperatures as low as 1°C, they are most commonly caught in bottom water temperatures ranging from 3.5 to 4.5°C (Compagno, 1984; Jakobsdóttir, 2001).

Overall, black dogfish is recorded at depths between 180-2250m (IUCN, 2009), while in West Greenlandic waters these were recorded and caught in large quantities at especially 500 and 1300 m depths (Yano, 1995). Hence, black dogfish are common in the mesopelagic zone (i.e. twilight zone) and in shallower parts of the bathypelagic zones, and live a part of their life in complete darkness, cold temperatures, and under high hydrostatic pressure (Treberg and Speers-Roesch, 2016).

Yano (1995) found evidence of a depth segregation by both size and maturity in black dogfish. In West Greenland waters small immature individuals are generally captured at shallow depths, and large mature individuals are caught at greater depths (Yano, 1995). In a study by Jakobsdottir (2001) females were found to outnumber males in the deeper waters, which could indicate a reproduction-related migration (Yano, 1995; Clarke et al., 2001; Jakobsdottir, 2001). This pattern was also found in other deep-water dogfishes (i.e. *Etmopterus princeps* and *Centrophorus squamosus*) (Jakobsdottir, 2001; Clarke et al., 2001). Differently, in Canadian waters pregnant females are reported to migrate to shallow depths (400m) of the Laurentian Channel when pupping (Kulka, 2006). Young specimens then move to greater depths of the channel, and further on to the slopes after reaching maturity (Kulka, 2006). A whole other pattern than that of the black dogfish living west of Greenland, where juveniles of all sizes are found in slope waters (Yano, 1995). Kulka (2006) suggest that the Greenlandic and Canadian stocks may be two separate stocks, despite a common distribution between them. This has never been investigated further.

1.3 Life history characteristics

Like other elasmobranch species, black dogfish is characterized by a K-selected life-history strategy, signified by slow growth, low fecundity, low natural mortality, fewer offspring, high longevity and late age at maturity (Cortes 2000; Stevens et al., 2000; Bublely et al., 2012; Matta et al., 2017). Having a low K value makes them more prone to over-exploitation by fisheries than fish with a high K value, especially if specimens are removed before maturation (Stevens et al., 2000; Bublely et al., 2012; Goldman et al., 2012; Jorgensen et al., 2014).

1.3.1 Growth pattern

Variation in life-history trait, including natural mortality, age at maturity, offspring size, and fecundity, is correlated with body size (Stevens et al. 2000). Indeterminate growth (i.e. maturation before attaining maximum size), sexual dimorphism, with females being the largest sex, and sex-specific growth rates are apparent for many fishes and sharks including the black dogfish (Compagno, 1984; Yano, 1995). Growth in marine organisms is estimated by the von Bertalanffy growth function (VBGF) (von Bertalanffy, 1938; Beverton and Holt, 1957; Ogle and Isermann, 2017). Hence, a difference in asymptotic length of females and males is reflected by L_{∞} in the VBGF (Figure 2), suggesting that females and males are not necessarily of similar age even though they are of the same length.

1.3.2 Age and size at maturity

Reproductive output in elasmobranch species increases with size and age (Stevens et al, 2000). Hence, fish and sharks are generally maturing at lengths corresponding to 65-80 % of maximum length (Beverton and Holt, 1959, Nielsen, 2013), and litter size have shown to increase with maternal size in e.g. gummi sharks (*Mustelus antarcticus*, Walker et al., 1998). A change in growth rate over time could be caused by length-selective fishing mortality which would affect the age and size structure of populations in complex ways (Walker et al., 1998). In case of small reproductive potential, only limited fishing mortality is sustainable, which makes knowledge of growth and age crucial for determine the sensitivity to fisheries, even for a by-catch species.

1.3.3 Longevity and natural mortality

Natural mortality is the removal of fish or elasmobranchs from the stock due to natural causes as e.g. competition, diseases, old age, predation and pollution (Fuiman and Werner, 2009; Matta et al., 2017). However, mortality associated with fishing is denoted a fishing mortality. These two combined provides the total mortality expected by a population (Matta et al., 2017). Natural mortality is one of the most difficult parameters to estimate, but also a critical element in studies of population dynamics (Jennings et al., 2009), why parameters such as growth rate, age and size at maturity (i.e. relatively simple measurements) are used as surrogates for natural mortality (Campana, 2001; Jennings et al., 2009; Buble et al., 2012). Maximum observed age may get underestimated and therefore not always represent the longevity of a species accurately, even though it is commonly reported. As fishing mortality increases, longevity tends to get underestimated due to small sample sizes of older individuals (Matta et al., 2017). The Greenland shark has an astonishing longevity of at least 272 years (Nielsen et al., 2016), but also longevity in the spiny dogfish has been estimated to between 80 and 100 years (Campana et al., 2006).

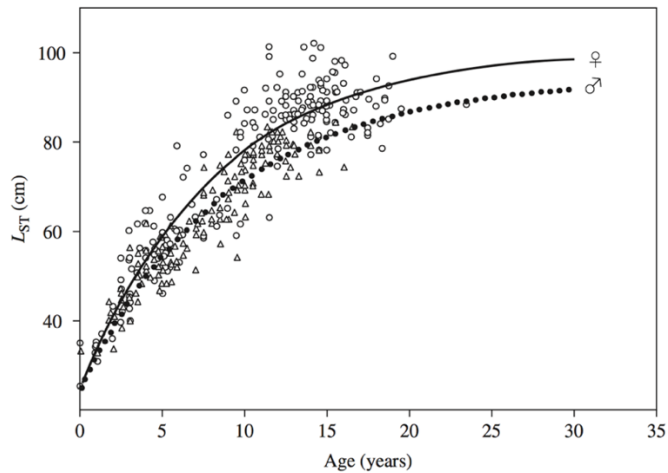


Figure 2 von Bertalanffy growth function of Spiny dogfish (*Squalus acanthias*) (Bublely et al., 2012).

1.4 Estimation and validation of age in elasmobranchs

Age determination allows for an estimation of key life history parameters related to natural mortality, growth and longevity (Goldman et al., 2012; Taylor et al., 2013; Matta et al., 2017) and is therefore crucial for the understanding of the biology of a certain species.

Age estimation of fishes generally relies on calcified “hard” structures that grow continuously throughout a life time and do not degenerate. This includes otoliths, scales, and bones (Campana and Torrold, 2001; Mendoza, 2006, Jennings et al., 2009). Elasmobranch species lack these hard structures as they have a soft cartilage skeleton and continuous replacement of teeth, which makes it difficult to estimate their age (Campana et al., 2006; Goldman et al., 2012; Taylor et al., 2013). However, age estimation has proven successful in elasmobranch species, when relying on tissue with a deposition of growth layers, such as vertebral center, caudal thornes, neural arch and fin spines (Cailliet et al., 2006; Campana 2006; McPhie and Campana 2009; Goldman et al., 2012; Matta et al., 2017).

For dogfish the traditional way for estimating the age has been based on dorsal fin spines (McFarlane and Beamish, 1987; Goldman et al., 2012; Taylor et al., 2013) and several studies have been made throughout time. The spine terminology described in these studies are quite dissimilar, making it difficult to maintain an overview. A study by Clarke and Irvine (2006) presents a guide to simplify the terminology, aiming to standardize the definitions and terms of the dorsal fin spine. This standardization was recommended by both Goldman et al. (2012) and Cotton et al. (2014) and was therefore used in this study together with a description of the construction of the dorsal fin spine from Beamish and McFarlane (1985).

1.4.1 The dorsal fin spines

A dorsal fin spine is triangular and consist of three major structural components; the internal pulp cavity filled with cartilaginous tissue, the stem (i.e. the main body of the spine) and the cap (i.e. the anterior dentine portion) (Figure 3A, Beamish and McFarlane, 1985; Tanaka, 1990; Clarke and Irvine, 2006). The spine grows at three distinct places; 1) externally from the base of the spine as a result of continuous deposition of dentine, 2) internally along the pulp cavity and 3) at the base of the cap (Figure 3B, Beamish and McFarlane, 1985, Cotton et al., 2014). The cartilaginous tissue supporting the spine is connected to the cartilaginous support of the dorsal fin and is produced at the spine base (Figure 3B). It is made up by chondrocytes and degenerates towards the tip of the spine. The posterior side of the spine is thinner than the anterior-lateral sides. The cap covers the anterior part of the spine distal to the dogfish. At the surface of the cap and the stem, darkly pigmented bands appear demonstrated to be growth bands (Beamish and McFarlane, 1985). Sections of the stem consists of three layers of dentine; inner, middle and outer (Figure 3C) (Tanaka 1990; Clarke and Irvine, 2006), and growth bands are present in all dentine layers (Figure 3C). However, the number of growth bands have shown to be greater in the inner dentine layer, than in the middle and outer dentine layers (Tanaka, 1990). Maximum counts of growth bands have been observed proximal to the constriction of the internal pulp cavity (Clarke et al., 2001; Beamish and McFarlane, 1985). According to Clarke and Irvine (2006) it is unknown if spines shrink when dried and suggest that all of these are measured even before or after drying or both. Growth bands are deposited annually, with a dark and a light growth band representing an annulus (Yigin and Ismen, 2016; Matta et al., 2017).

The traditional method of estimating the age of particularly spiny dogfish has been to count growth bands visible on the surface of the second dorsal fin spine, since the first dorsal fin spine tend to be more damaged and worn down (Beamish and McFarlane, 1985; Goldman et al., 2012; Yigin and Ismen, 2016). Spines are formed during embryonic development and pups have spines at the time of birth (Soldat, 1982), making it possible to investigate the age of all size classes. Spines grow externally on the body, making it possible to collect them nonlethally (Cotton et al., 2014). However, because of this, they often become subject to breakage and natural wear throughout life, which might lead to missing annuli (Bublely et al., 2012; Cotton et al., 2014). Especially, in large dogfish, age readings can be difficult to achieve due to surface damage or close location of annual growth bands (Yigin and Ismen, 2016). Calculations have been developed in order to correct for missing annuli (Goldman et al., 2012). A lack of correction could lead to an underestimation of age and therefore wrongful conclusion on lifespan, growth rate and age-at-maturity (McFarlane and Beamish, 1987) Growth bands on the dorsal fin spines can be made visible by wet-sanding and polishing the surface, to remove

pigment and enamel (Goldman, 2012). However, growth bands do not always appear on the surface, why also cross-sections have proven useful for age estimation (Soldat, 1982; Clarke, 2001).

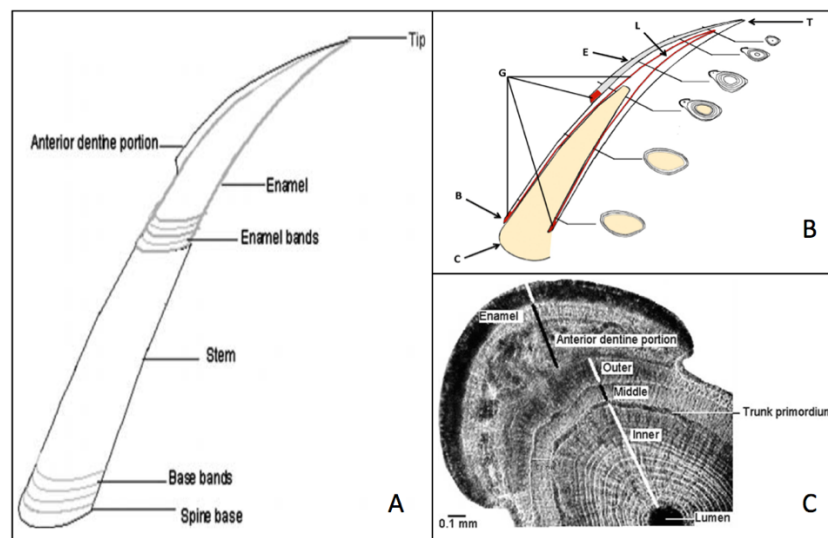


Figure 3 Structures of a dorsal fin spine. A: External structures (Clarke and Irvine, 2006). B: Conceptual model of growth, indicating the spine tip (T), spine lumen (L), cap (E), spine growth zones with deposition of new dentin and enamel (G, in red), spine base (B) and internal cartilage support (C) (Cotton et al., 2014). C: Cross section of the spine, showing the internal structures (Clarke and Irvine, 2006).

1.4.2 Radiocarbon dating

The credibility of age estimates relies on validation, where one of the strongest and most frequently used form of validation is bomb radiocarbon dating (Campana et al., 2006; Matta et al., 2017). Bomb radiocarbon dating uses the properties and incorporation of ^{14}C into metabolic inactive structures to determine how long it has been since a given sample stopped exchanging carbon; the older the samples the smaller the amount of detectable ^{14}C (Goldman et al., 2012).

Carbon appears as two stable isotopes (^{12}C and ^{13}C) and one unstable, and hence radioactive, isotope; ^{14}C . The approximate ratio is 100:1:1.1*10⁻¹² respectively (Van der Merwe, 1982). Radiocarbon is formed in the stratosphere from high-energy neutrons and nitrogen molecules (i.e. by emission of a proton) and will eventually decay to nitrogen and stable carbon isotopes (^{12}C), making the amount of ^{14}C vary naturally (Libby, 1960). Carbon is the most fundamental building block of living organisms and isotopes are distributed in the ocean as dissolved inorganic carbon (DIC) and as CO_2 across the atmosphere (Kalish, 1993). Carbon isotope profiles are transferred across the food web, as carbon of autotrophic and heterotrophic organisms is exchanged through photosynthesis/ingestion and respiration continuously.

In 1963, ^{14}C amounts almost doubled in the atmosphere and increased in both marine and terrestrial environment, all over the world, due to atmospheric testing of thermonuclear bombs in the late 1950's and early 1960's (Kerr et al., 2006; Scourse et al., 2012; Hamady et al., 2014). Within a short period of time, this very specific increase in radioactive carbon was incorporated in all organic tissue which created a distinct “bomb-pulse”, making this period a fixed dated marker (Campana et al., 2002; Campana et al., 2006; Scourse et al., 2012; Nielsen et al., 2016, Figure 4). Due to ceasing of substitution and remodeling of carbon molecules in metabolic inactive structures, ^{14}C only undergoes radioactive decay. As ^{14}C decays at a known rate (half-life of 5730 years, Libby, 1960), the proportion of radiocarbon incorporated into tissue as shells, spines, calcified vertebra and eye lenses can be used as bioenergetics archives of the ^{14}C chronology of the surrounding marine environment (Bowman, 1990; Kalish, 1993; Campana et al., 2002; Campana et al., 2006; Nielsen, 2013). Higher values of ^{14}C was found in organisms from the post-bomb era compared to those from the pre-bomb era and according to Scourse et al., (2012) and 95 percent modern carbon (pMC) have shown to be the threshold for the presence or absence of a bomb-pulse.

Kalish (1993) was the first to demonstrate the applicability of bomb radiocarbon as a validation method of age estimations of fish in New Zealand. In 2002 Campana et al. reported the first application of bomb radiocarbon as an age validation method for long-lived sharks, based on date-specific incorporation of radiocarbon into vertebral growth bands of porbeagle (*Lamna nasus*). Their results indicated that vertebrae preserved a bomb radiocarbon pulse in growth bands formed during the 1960s. Additionally, he was the first to report the application of bomb radiocarbon as an age validation method based on date-specific incorporation into dorsal fin spines of spiny dogfish (Campana et al., 2006). Recently Nielsen et al (2016) was the first to use this technique on eye lens nuclei to identify the bomb pulse for validating age of the Greenland shark (*Somniosus microcephalus*), which is the technique used in this study as well.

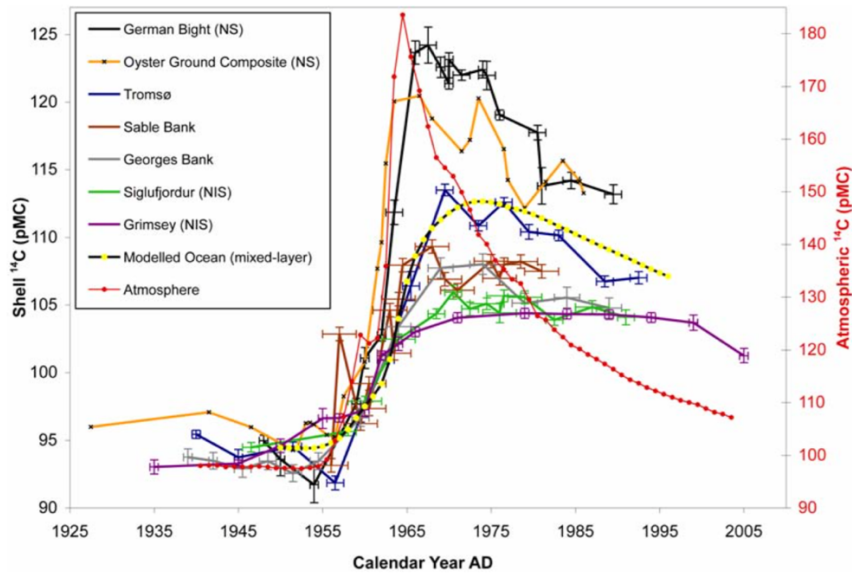


Figure 4 Percent modern carbon of ^{14}C (pMC) in shells from different sites plotted against atmospheric ^{14}C (pMC, Scourse et al., 2012).

Validation of age estimates is based on timing of the ‘bomb pulse’ in the marine environment as values of ^{14}C are reduced with depth and the incorporation of ^{14}C is related to ocean circulation and mixing. The bomb pulse has been established as a chemical time marker (Williams, 1987; Kerr et al., 2006). Different reservoirs (i.e. the atmosphere, surface waters and deep ocean waters) measure different radiocarbon reservoir ages. The ocean mixed waters are in average 400 years older than the atmosphere in respect to ^{14}C (Bowman, 1990) due to upwelling and mixing of very old ^{14}C depleted deep water with the surface waters and a delayed exchange rate between oceanic carbonate and atmospheric CO_2 . The reservoir age varies between different areas due to especially topography and wind patterns (Bowman, 1990).

1.4.3 The eye lens

To understand the use of eye lenses for validation of age estimation, it is necessary to understand its components and development. Black dogfish eye lenses, as with all other vertebrate eye lenses, are composed of three main parts; lens fibers, lens epithelium and a lens capsule (Cohen 1965). Lens fibers, the building blocks, are making the nucleus of the eye lens dense by being firmly packed. The lens epithelium is located in the anterior portion of the lens between the capsule and the fibers, serving as an originator of new lens fibers. The lens capsule is a transparent membrane with high elasticity surrounding the entire lens. Furthermore, the center of the nucleus is made of primary lens fibers and is referred to as the embryonic nucleus (Taylor et al. 1996). The surrounding fibers are secondary lens

fibers added continuously in concentric layers throughout the life of the organism (Taylor et al. 1996). The embryonic nucleus is visible to the naked eye, because primary lens fibers are not arranged in concentric layers and therefore appear different from the secondary lens fibers.

When an embryo is created, the food consumed by the mother forms the basis of the material incorporated into the embryo's eye nucleus. The tissue in the nucleus is metabolically inactive, isolated and filled with crystalline proteins, why protein synthesis, DNA replication and RNA transcription cannot be carried out, making the nucleus among the oldest parts of the organism (Bassnett et al., 2011). Therefore, the composition of the nucleus reflects the diet of the mother and thus the surrounding water's chemical signature at the time of formation. This gives the nucleus some unique biological characteristics making it suitable for age validation purposes.

Reconstruction and interpretation of the radiocarbon chronology depends on the determination of an organism's trophic position and feeding ecology, in this case the diet of the mother at the time of nucleus formation. Based on the principle that heavier isotopes (^{13}C and ^{15}N) accumulate from prey to predator (i.e. diet-tissue enrichment Δ), stable isotope analyses of carbon and nitrogen isotopes ($\delta^{13}\text{N}$ and $\delta^{15}\text{C}$) can provide valuable information on both the carbon source and the trophic position (Post, 2002; Hansen et al., 2012). A high $\delta^{15}\text{N}$ value indicates that nitrogen is derived from the highest trophic position in the food web, as values of predators typically are enriched by 3 to 4% compared to their food source (Post, 2002). Unlike otoliths in fish, which primary source of ^{14}C is derived from DIC (70-90%) obtained from ambient seawater and where only 10-30% is dietary, dogfish eye lenses reflect the ^{14}C composition of their mothers' diet (Campana et al., 2002; Kerr et al., 2006). An understanding of the food composition of a species is necessary for a better understanding of the ^{14}C values of the nucleus (Kerr et al. 2006).

1.5 Maturity and reproduction

Black dogfish have ovoviviparous (i.e. aplacental viviparous) reproduction, with internal development of eggs within the uterus of the female, hence giving birth to free-living young (Yano, 1995). During pregnancy, the embryo relies on the female for provision of oxygen and therefore the wall of the oviduct enlarges and becomes supplied with blood vessels. However, the embryos do not receive any nutrition from the female, but rely entirely on a yolk-sack in the egg (i.e. lecithotrophy), which is different from viviparous reproduction, where the embryos receive nutrition from the female (i.e. matrotrophy) (Wootton, 2012). The ovoviviparous reproduction strategy is quite conservative, with

fewer but larger offspring than oviparous (i.e. egg laying) species. Black dogfish can give birth to between 14 and 31 embryos (Qvist, unpublished data), while oviparous fish as an average mature female cod (*Gadus morhua*) produce up to 5 million eggs in a batch (ICES, 2004). A low fecundity combined with a possible late age at maturity makes black dogfish vulnerable to fisheries, suggesting that they may not sustain intensive exploitation. According to Yano (1995), no well-defined pupping season is recorded within the black dogfish in West Greenland waters.

This is the first known study to investigate the possibility of using fin spines for age determination in black dogfish. The aim of the study is to 1) estimate the age of black dogfish by counting growth bands in the spine of the second dorsal fin. 2) validate these estimates using radiocarbon dating on the embryonic eye lens nucleus. 3) to determine the distribution in Greenlandic waters from existing data and 4) define the size and age at maturity of black dogfish.

Jointly, this will contribute significantly to the biological knowledge on a little known, but widely distributed species that is vulnerable because of its frequent presence as by catch in commercial fisheries.

2 Material and methods

2.1 Sampling, survey

Yearly bottom trawl surveys in Greenland waters have been conducted by GINR since 1991 in West Greenland and 1998 in East Greenland, however, the survey in lower depths started only in 2008 (For survey description see Jorgensen et al. 2014, Fig. 1). An Alfredo trawl has been used continuously throughout the period at depths between 400 m and 1500 m, but a shift in gear at shallow depths (100-600m) was made in 2005 from a Skjervøy to a Cosmos trawl. These were considered to have similar catchability (GINR, unpublished data) and no corrections were applied to the catches. Combined, the surveys cover depths ranging from 328 and 1493 m with depths defined as the average trawl depth in a haul. I present black dogfish density estimates ($\text{kg}\cdot\text{km}^{-2}$), where these are based on swept area estimates, calculated as the difference between start- and stop-coordinates multiplied by the door spread. Bottom temperature was measured at most hauls. In total 5571 black dogfish were caught. Not all specimens were measured, but the total weight of black dogfish was registered in all hauls. Yearly catches in number, are given in Table 1, for both East and West Greenland.

Table 1 Yearly catches of black dogfish numbers from the eastern and western sampling sites of Greenland.

| Year | East (N) | West (N) |
|------|----------|----------|
| 1991 | | 151 |
| 1992 | | 4 |
| 1994 | | 83 |
| 1995 | | 11 |
| 1996 | | 18 |
| 1997 | | 125 |
| 1998 | 20 | 177 |
| 1999 | 236 | 142 |
| 2000 | 180 | 155 |
| 2001 | | 52 |
| 2002 | 94 | 172 |
| 2003 | 105 | 188 |
| 2004 | 103 | 145 |
| 2005 | 87 | 165 |
| 2006 | 385 | 60 |
| 2007 | 59 | 121 |
| 2008 | 116 | 111 |
| 2009 | 192 | 119 |
| 2010 | 152 | 113 |
| 2011 | 67 | 144 |
| 2012 | 133 | 108 |
| 2013 | 234 | 68 |
| 2014 | 196 | 152 |
| 2015 | 103 | 101 |
| 2016 | 239 | 185 |

2.2 Sampling & biological analysis

Between June and September 2016, 424 black dogfish were frozen at -20°C upon capture. At GINR 283 black dogfish were thawed at 5°C , sexed, measured to nearest cm below (total length, TL and standard length, SL) and weighed (g). Both dorsal fin spines were removed from black dogfish and eye lenses were dissected from the eye globes. All samples were individually bagged, labeled and stored frozen immediately after removal. Maturity stage was determined according to the categories defined in Yano (1995). The maturity of males was determined by the hardness of claspers and by presence/absence of sperm in the sperm sacks (i.e. hard claspers = mature, soft claspers = immature). Mature males were classified into one of four stages of maturation depending on the amount of sperm: (0) empty; (1) nearly empty; (2) moderate; (3) full. Females with small ovaries and threadlike uterus were classified as immature (IM), while all other females were classified as mature (M). The mature females were divided into six stages of maturation: (1) Developing ovaries with expanded uteri (>10 mm in width); (2) Ripe ovaries with expanded uteri (>10 mm in width); (3) Fertilized ovaries in the uteri; (4) Developing embryos with external yolk-sack; (5) Near-term embryos without external yolk-sack; (6) Post-partum, small ovaries and flaccid uteri (>20 mm in width).

2.3 Age estimation

2.3.1 Fin spine preparation

Age estimates in this study are based on the assumption that all bands were formed annually. Age estimates were based on the second dorsal fin spine of black dogfish, as this was both larger and often less damaged than the first dorsal fin spine. Spines were cleaned by soaking in hot water for a short period of time to remove connective- and cartilaginous tissue. All spines were measured (i.e. length and diameter in mm) after drying. Measurement of the diameter was made at the base of the spine. Band readings both externally and in the cross-sections were based on identification of a dark band followed by a light band, defined as an annulus and considered as constituting a year's growth. Spines from embryos were processed to determine whether or not the first growth band was laid down before birth. Moreover, a second dorsal fin spine from a spiny dogfish (*S. acanthias*) was processed using the same technique as for spines from black dogfish. The spine from the spiny dogfish was studied and aged as a reference to black dogfish.

2.3.2 External bands

Spine surfaces were wet-sanded and polished to remove damaged enamel and pigment to reveal band structures after which spines were photographed using a digital camera. The number of annuli were counted. Spines were baked in the oven (one hour at 200°C, Figure 5) and sectioned longitudinally (Figure 6).



Figure 5 Dorsal fin spine baked for one hour at 200°C



Figure 6 Longitudinal section of black dogfish.

2.3.3 Cross-sections

Spines were embedded in Epoxy (24 hours) before being sectioned transversely (500 μm) using a Struers Secotom-50 saw, with a diamond blade rotating at 4400rpm and 400mm/s. Sections were wet-sanded to remove saw blade marks and smoothen the surface. Sections were applied with a thin layer of oil to make bands even more visible, photographed and read. All growth bands visible were counted and used to estimate age. Spine length and diameter were plotted against dogfish length to determine if a correlation was significant. To ensure reproducibility and precision of the interpretation of age, all spine sections were read by three age readers. Counting was performed without knowledge of the other readers' band-counts or the length of the specimen. Bias between readers was evaluated with age bias plots, whereas the coefficient of variation (CV) was used to quantify precision between readers, using the following equation:

$$CV_j = 100\% * \frac{\sqrt{\frac{\sum_{i=1}^R (X_{ij} - X_j)^2}{R-1}}}{X_j}$$

Where CV_j is the precision of age estimate for the j th fish. X_j is the mean age estimate and R is the number of times each fish is aged.

The von Bertalanffy growth function (VBGF) was then fitted to the length-at-age data, for an estimation of size-at-age:

$$L_t = L_\infty(1 - e^{-K(t-t_0)})$$

where L_t is the expected length at age t , L_∞ is asymptotic maximum length, K is the growth rate towards the asymptotic length and t_0 is the theoretic age at zero length (Bertalanffy, 1938).

Longevity was estimated using the equation:

$$A_{95} = t_0 - \left(\frac{\log_e(1-0.95)}{K}\right)$$

Where A_{95} is the time (in years) passed before reaching 95% of L_∞ and K is the growth rate derived from the von Bertalanffy growth equation (Fabens, 1965).

2.4 Radiocarbon analysis

2.4.1 Eye lens preparation

To validate the age estimations based on spine sections for black dogfish, radiocarbon of primary fibers in eye lenses was analyzed. Ten specimens were analyzed for percentage modern carbon (pMC). This included five small individuals (<19cm) and five large individuals (>76cm) (Table 3, under the results). The eye lens removal procedure is shown in figure 7. First step after removing the eye lens was to expose and isolate the lens nucleus by rolling it onto a piece of paper, to remove the outer cortex and lens capsule. Secondary lens fibers were removed under a stereomicroscope, using tweezers and a scalpel to isolate the embryotic nucleus. Samples of embryotic nuclei were dissected to weigh 10 mg, after which 4 mg were used for bomb radiocarbon (¹⁴C) analysis, while the rest were used for stable isotope analyses (see the next section). Samples of organic carbon were combusted with CuO (950°C) in vacuum-packed combustion tube, resulting in CO₂. Sampled CO₂ was submitted for graphitization followed by accelerator mass spectrometry (AMS).

Radiocarbon content was quantified in order to identify the presence/absence of a bomb pulse with AMS. The results of the radiocarbon dating are reported according to international convention (Stuvier and Polach 1977), and the pMC is based on the measured ¹⁴C/¹³C ratio. With a value larger than 95 pMC, a bomb pulse is considered present, (Scourse et al. 2012). The results have been normalized to a standard δ¹³C value of -25‰, correcting for the natural isotopic fractionation effect (δ¹³C calibration standard, Stuvier and Polach, 1977).

2.4.2 Stable isotope analysis

Stable isotopes were used for identifying the carbon source of the embryotic nucleus, by quantifying ¹³C and ¹⁵N with a high-precision stable-isotope mass spectrometry. Ratios are expressed in conventional δ notation in parts per thousand (‰) using;

$$\delta X = \left[\left(\frac{R_{sample}}{R_{standard}} \right) - 1 \right] * 1000$$

where X is ¹³C or ¹⁵N and R is the ratio of the heavy to light isotopes (¹³C/¹²C or ¹⁵N/¹⁴N). δ¹³C and δ¹⁵N were measured on a GV Instruments IsoPrime Stable Isotope Mass Spectrometer to a precision of 0.2‰.

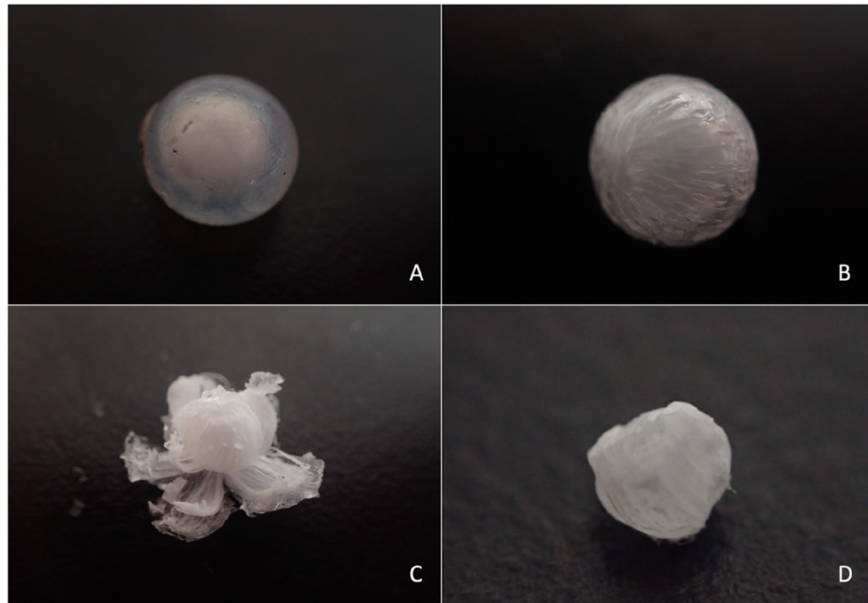


Figure 7 Eye lens from Black dogfish. A: Eye lens with outer membrane. B: Secondary lens fibers, growing in concentric layers. C: Removing of the secondary lens fibers. D: Embryonic nucleus consisting of primary lens fibers.

2.5 Distribution

Two geographical areas were defined based on the distribution of catches of black dogfish: ‘East’ (East of 44°W) and ‘West’ (West of 44°W, Figure 17). The density of captured dogfish within these areas were evaluated in intervals of 200 kg*km⁻². Distribution of sex, length and depth of capture were analyzed (table 4). The relationship between density and bottom temperature was assessed.

2.5.1 Biological information

A length-weight relationship was fitted for ‘East’ and ‘West’ combined, but for each sex separately:

$$W = a * TL^b$$

where W represents total weight (kg), L represents total length (cm), and a and b are constants. Maturity ogives were fitted for both sexes using a binary model (R package) with maturity defined as either immature or mature based on the definition given in Yano (1995). The lengths at maturity (L₅₀) was estimated for each sex.

3 Results

3.1 Age estimation

Of the 283 spine samples collected from black dogfish, 49.6% (N = 141) were processed and photographed. Seventy-three were females and 68 were males. The only usable spine sample of spiny dogfish was from a male of 81cm. It originated from the North Sea, but was caught as a by-catch in the fishery, why it ended up living in captivity for a short period of time (i.e. a few months to a few years (Pers. Obs. Rune Kristiansen)).

3.1.1 External bands

The exposed part of the second dorsal fin spines from spiny dogfish was covered with enamel and had visible growth bands on the surface, while the part embedded in the body was whitish and exhibited no obvious band structures (Figure 6A). The bands appeared clearer after removing enamel and pigment on the surface of the spine by wet-sanding and polishing. Unlike the spines of spiny dogfish, the spines of black dogfish were not covered with enamel (Figure 6B). Instead the spine was whitish, almost transparent, without any bands. Band structures were impossible to make visible by wet-sanding and/or polishing (Pers. Obs.).

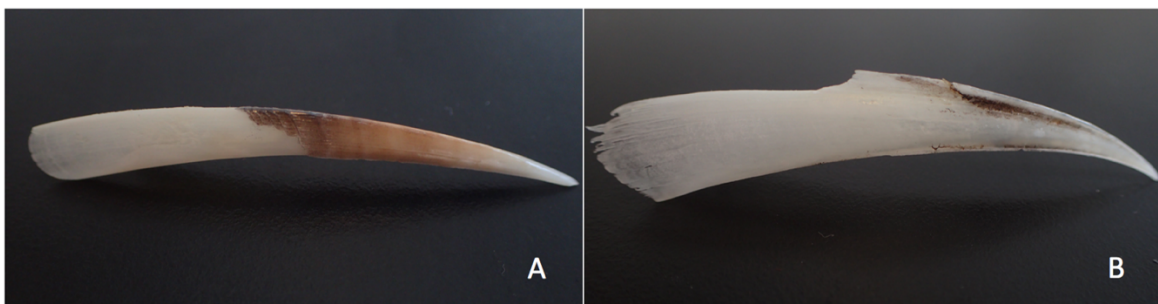


Figure 8 External structures of the second dorsal fin spine of (A) Spiny dogfish (*S. acanthias*, 6.3mm) and (B) Black dogfish (*C. fabricii*, 6.5mm).

3.1.2 Cross-sections

Spines sectioned without any kind of stabilization would break because of their porosity and thinness, which made them useless for age estimation. Sections were obtained distal to the constriction of the internal pulp cavity. These sections often delivered a better visibility of growth bands than sections from other parts of the spine (Figure 9). Still this varied between spines. The lack of visibility in cross-sections made it difficult to determine which section showed the maximum counts of growth bands and sections were chosen based on their visibility. Furthermore, breakage of spines made it sometimes impossible to obtain a proper cross-section and therefore the possibility to obtain a maximum count of

growth bands was low in these spines. Far from all cross-sections had a clear division of inner, middle and outer dentine, instead most sections had a more or less homogeneous appearance (Figure 10A, B and C). This was quite different from cross-sections of a dorsal fin spine from the spiny dogfish, showing a clear division of inner, middle and outer dentine (Figure 10D). Frequent breakage or wearing, little spacing between growth bands or low visibility of growth bands was often found in sections from the largest dogfish. Spines obtained from the smallest dogfish were easier to break than the others, making processing of these difficult.

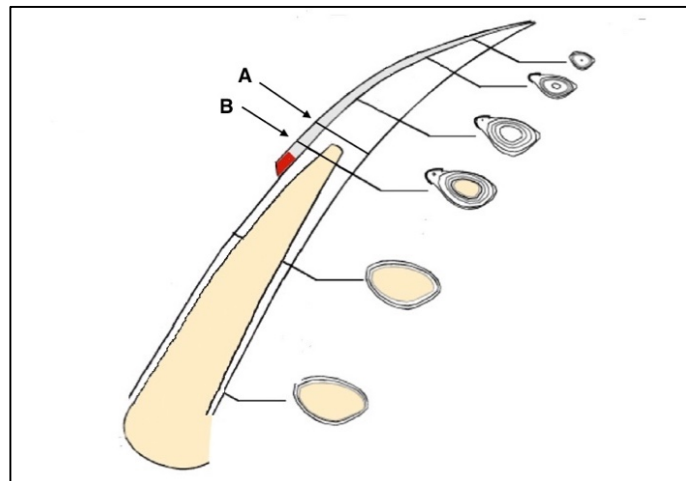


Figure 9 Model of dorsal fin spine sectioning, A: proximal to the constriction of the internal pulp cavity, used in previous studies and B: distal to the constriction of the internal pulp cavity, used in this study.

Of the 141 sections photographed, 85% (N = 120) were read. Spine sections were grouped into three groups, dependent on the ease of reading; group 1) sections that were easy to read (N = 38, Figure 10A and B), group 2) sections that was read with difficulties (N = 50) and group 3) unreadable sections (N = 32, Figure 10C). Group 1 and 2 was used for age estimations, while group 3 was discarded. Readings of the cross-sections from spiny dogfish gave an estimated age of approximately 18 years (Figure 10D). The age estimates of black dogfish are presented in appendix I.

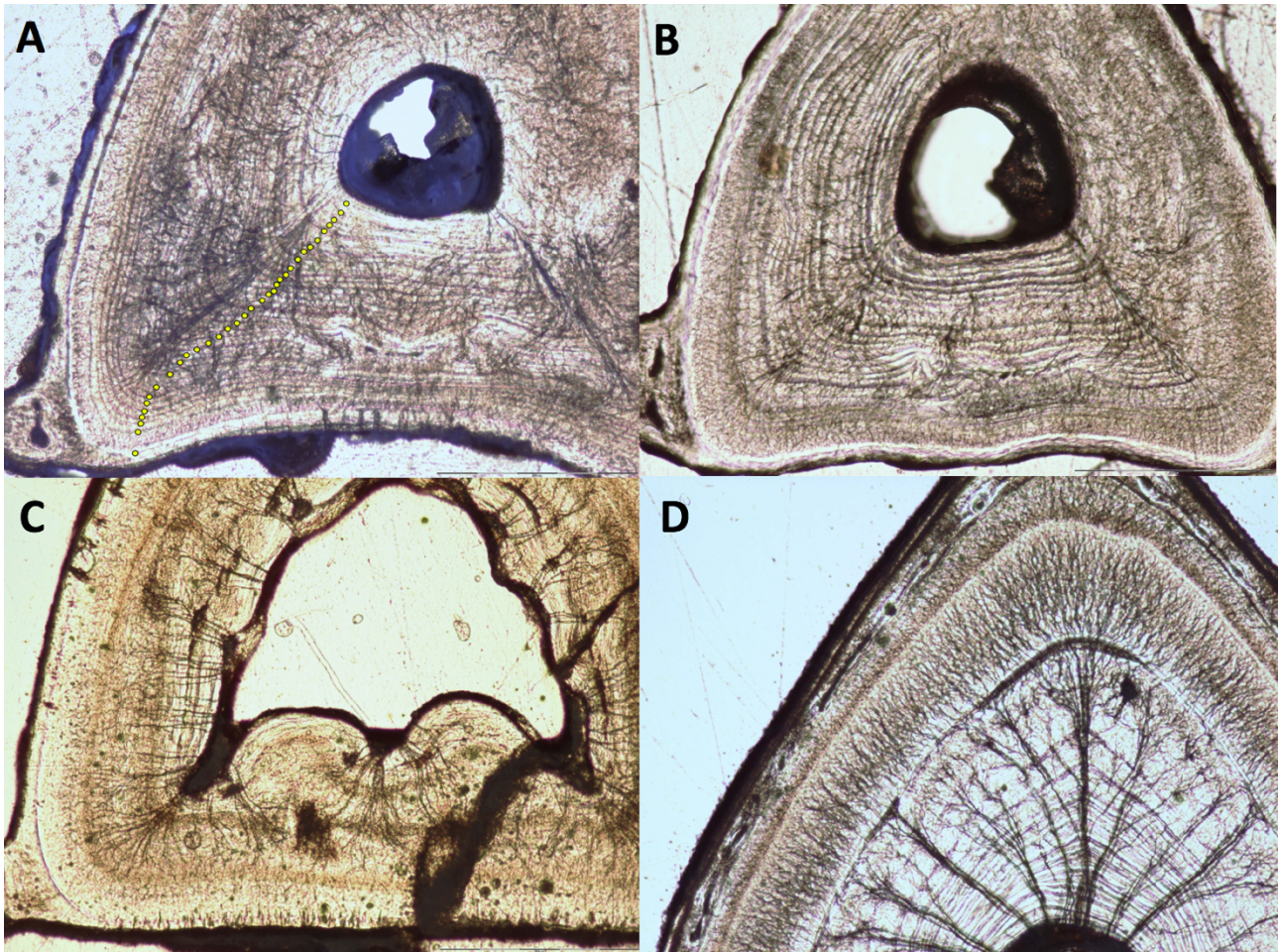


Figure 10 Cross section of black dogfish. A and B: Easy read section, B: Unreadable section, D: Cross section of spiny dogfish.

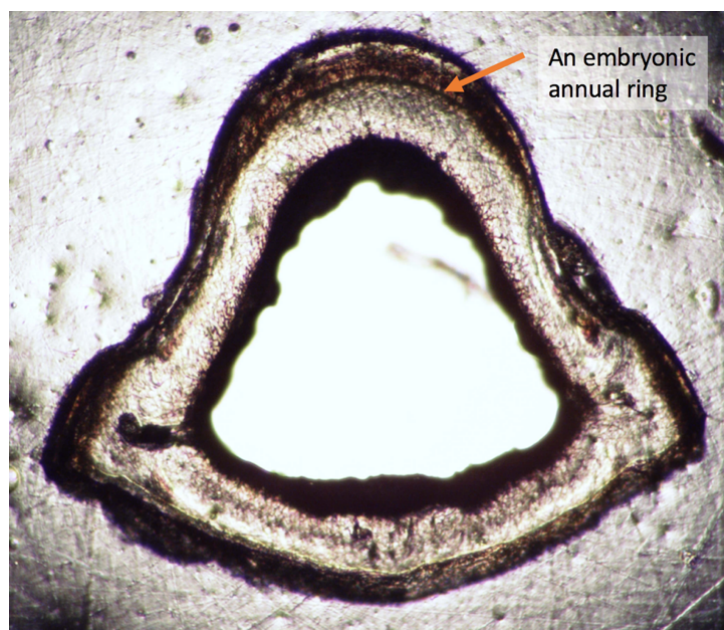


Figure 11 Embryonic cross-section showing the first annual ring.

The VBGF show a difference in growth pattern between sexes (Figure 12, Table 2). The asymptotic length (L_{∞}) was greater for females (96) than that of males (75). The growth rate (K) was however smaller for females (0.039) than for males (0.049). Estimated longevity (i.e. the age at which black dogfish reaches 95% of their maximum size) is 73 years for females and 57 years for males. However, in this study the oldest individual has an estimated age of 38 years for females and 37 years for males (Appendix I). Maximum growth band readings for reader 1 was 41, while it for reader 2 was 46 and for reader 3 was 41.

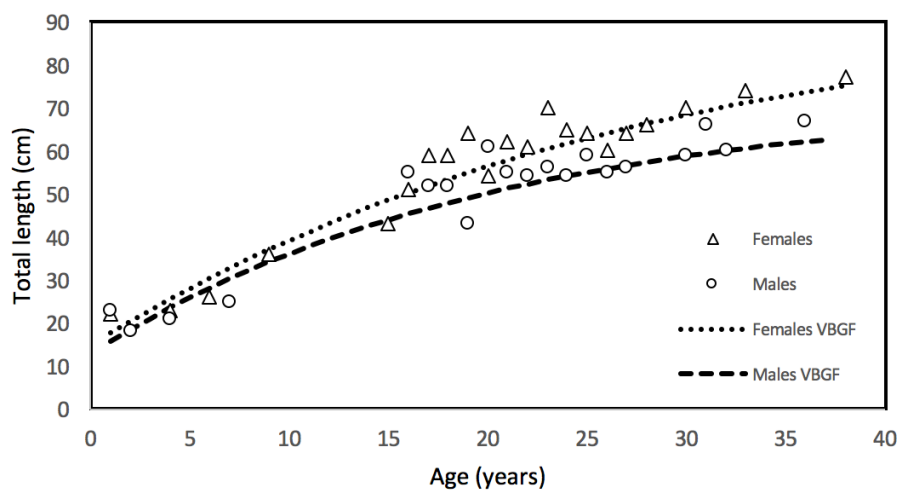


Figure 12 von Bertalanffy growth function (VBGF) in total length (TL) of females (. . . .) and males (- - - -) of black dogfish, based on age estimates for females (Δ) and males (O) obtained from sectioned fin spines.

Table 2 von Bertalanffy growth parameters and longevity (A_{95}) for females and males, as well as for both sexes combined.

| Sex | L_{∞} (cm) | K (year^{-1}) | T_0 (year) | A_{95} (years) |
|-----------------|-------------------|----------------------------|--------------|------------------|
| Females | 96 | 0.039 | -3.9 | 73 |
| Males | 75 | 0.049 | -4.05 | 57 |
| Combined | 86 | 0.04 | -3.7 | 71 |

Analyses show that both spine length and diameter increase linearly with body size (Figure 13). The best correlation was found between dogfish length and spine length ($r = 0.94$). Due to frequent breakage or wearing down of spines from especially large dogfish, the most broken or worn down spines have been removed from the dataset and has not been accounted for in the correlation (Figure 13). Minimum spine length was 10 mm from 180 mm dogfish, while maximum spine length was 65 mm from a dogfish of 770 mm. Spine width was measured at a minimum of 2 mm from dogfish with lengths between 170 and 250 mm, while maximum spine width was of 12 mm from dogfish with lengths between 610 and 770 mm.

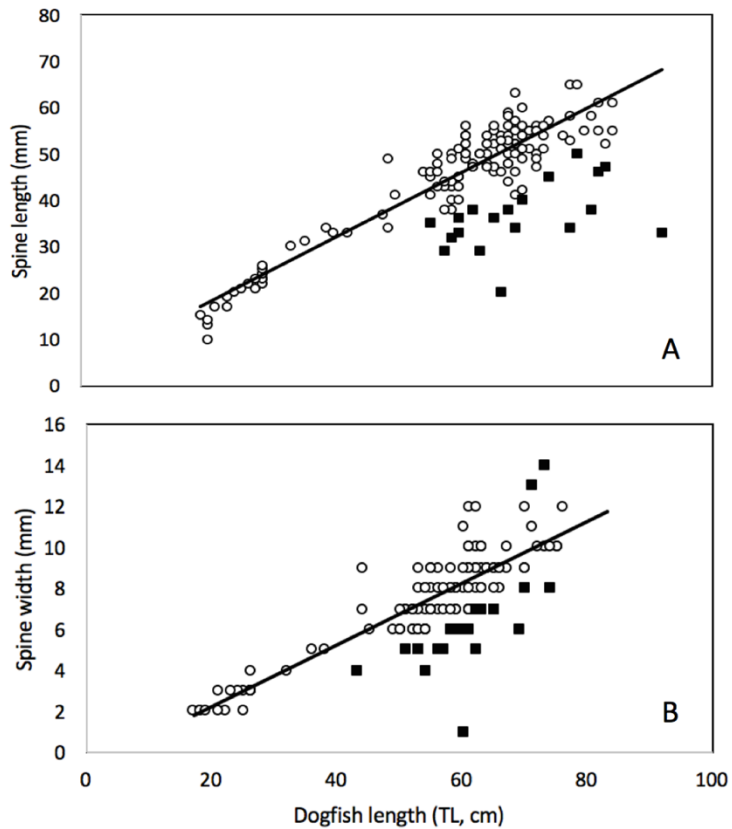


Figure 13 Correlation between (A) dogfish length and spine length, and (B) dogfish length and spine diameter at its base. Squared points indicate rejected data.

Age bias plots showed some variation around a 1:1 line and a slight systematic over- or underestimation of age (Figure 14). The coefficient of variation (CV) was 8% on average (11% for reader 1, 7% for reader 2 and 6% for reader 3, based on three readings from reader 1 and 2, but only two readings from reader 3). Minimum and maximum CV for reader 1 was 0 and 30, while it for reader 2 was 0 and 17 and for reader 3 was 0 and 28. Frequency CV indicates a high level of reproducibility in readings based on spine sections (Figure 15).

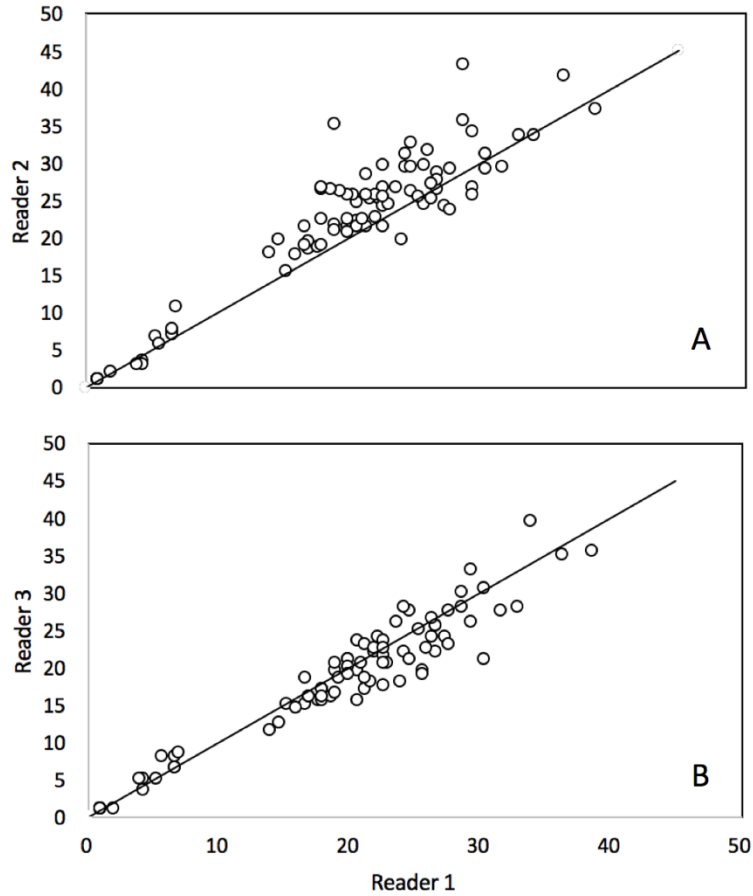


Figure 14 Bias plot between the primary (1), secondary (2) and tertiary (3) readers of age estimates of black dogfish using second dorsal fin spines. The primary and secondary readers read 87 cross-sections from second dorsal fin spines, while the tertiary reader read 84.

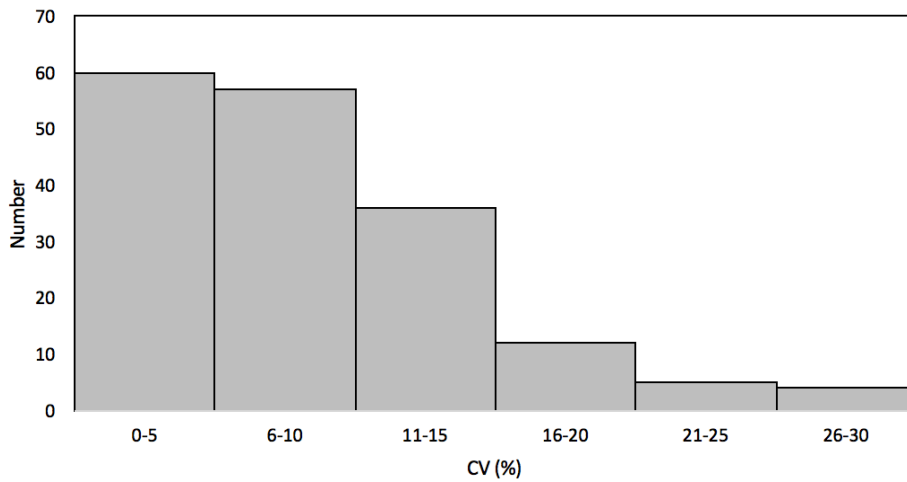


Figure 15 Frequency histogram of coefficient of variation (CV) for annual age estimates from the second dorsal fin spine.

3.2 Radiocarbon analysis

Table 3 Summary of samples collected for radiocarbon analysis and stable isotopes from embryonic nuclei from both the eastern and western areas of Greenland.

| Dogfish ID | TL (cm) | Area | pMC \pm SD | $\delta^{13}\text{C}$ \pm SD | $\delta^{15}\text{N}$ \pm SD | Estimated age (years) from the VBGF |
|------------|---------|------|-------------------|--------------------------------|--------------------------------|-------------------------------------|
| 284 | 16 | W | 103.84 \pm 0.32 | -16.98 \pm 0.1 | 11.11 \pm 0.22 | Embryo |
| 199 | 17 | W | 103.61 \pm 0.45 | -17.77 \pm 0.1 | 10.22 \pm 0.22 | 1 |
| 200 | 18 | W | 103.1 \pm 0.35 | -17.15 \pm 0.15 | 11.02 \pm 0.33 | 1 |
| 207 | 18 | W | 104.14 \pm 0.38 | -17.35 \pm 0.15 | 11.11 \pm 0.33 | 1 |
| 212 | 18 | W | 105.65 \pm 0.4 | -17.25 \pm 0.15 | 9.97 \pm 0.33 | 1 |
| 223 | 77 | E | 93.79 \pm 0.32 | -16.14 \pm 0.1 | 12.24 \pm 0.22 | 38 |
| 025 | 77 | E | 93.48 \pm 0.33 | -16.42 \pm 0.15 | 11.67 \pm 0.33 | 38 |
| 273 | 78 | E | 93.41 \pm 0.47 | -15.92 \pm 0.15 | 12.17 \pm 0.01 | 39 |
| 251 | 83 | E | 93.18 \pm 0.34 | -16.25 \pm 0.15 | 10.03 \pm 0.33 | 47 |
| 88 | 83 | E | 93.54 \pm 0.3 | -16.47 \pm 0.15 | 10.38 \pm 0.33 | 47 |

All the radiocarbon analyses were successful. All the small individuals had radiocarbon values above 100 pMC, which is consistent with the post-bomb period. All the largest individuals have pMC values below 95 pMC, which is consistent with the pre-bomb period (Figure 16). Unfortunately, most of the spines from the largest dogfish were damaged and worn down to such an extent that it was impossible to estimate an age for these individuals based on cross sections. These were however estimated from the VBGF (Table 3).

The values of $\delta^{13}\text{C}$ ranged between $-15.92 \pm 0.15\text{‰}$ and $-17.35 \pm 0.15\text{‰}$ (mean \pm SD, t-test, t-value= 6.40, p-value < 0.01, Table 3) with an overall mean of $-16.77 \pm 0.14\text{‰}$ (\pm SD). Eye nuclei from larger dogfish had less depleted values than those of small dogfish (Figure 17). Values of $\delta^{15}\text{N}$ ranged between $9.97 \pm 0.33\text{‰}$ and $12.24 \pm 0.22\text{‰}$ (mean \pm SD, Table 3) with no significant difference between eye nuclei from small and large dogfish (t-test, t-value= 1.18, p-value = 0.2832, Figure 17).

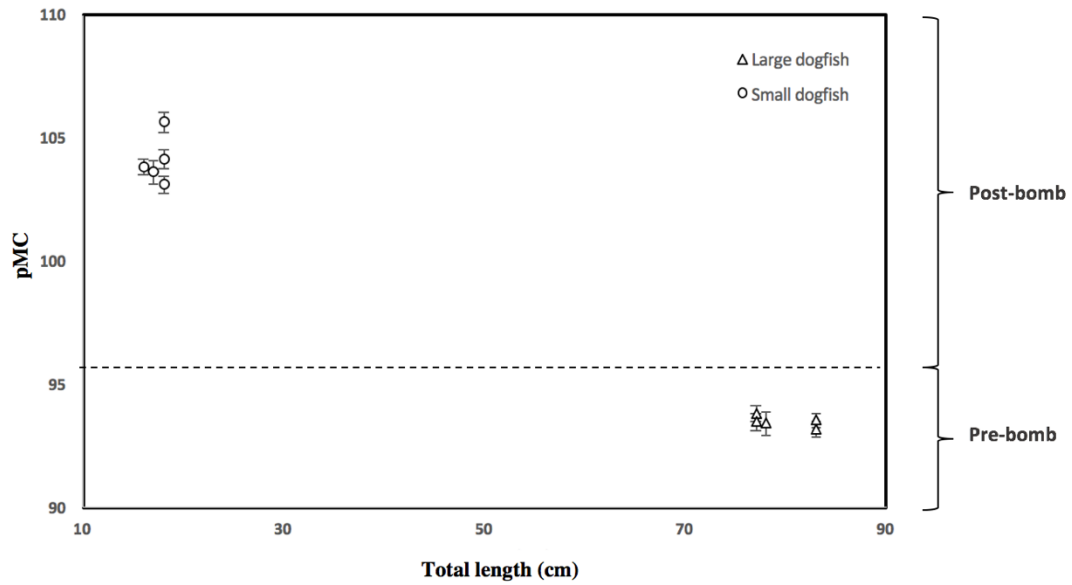


Figure 16 Mean pMC \pm SD (14C level) values from eye lenses of 10 dogfish. Dotted line indicates threshold value for a bomb pulse (>95 pMC).

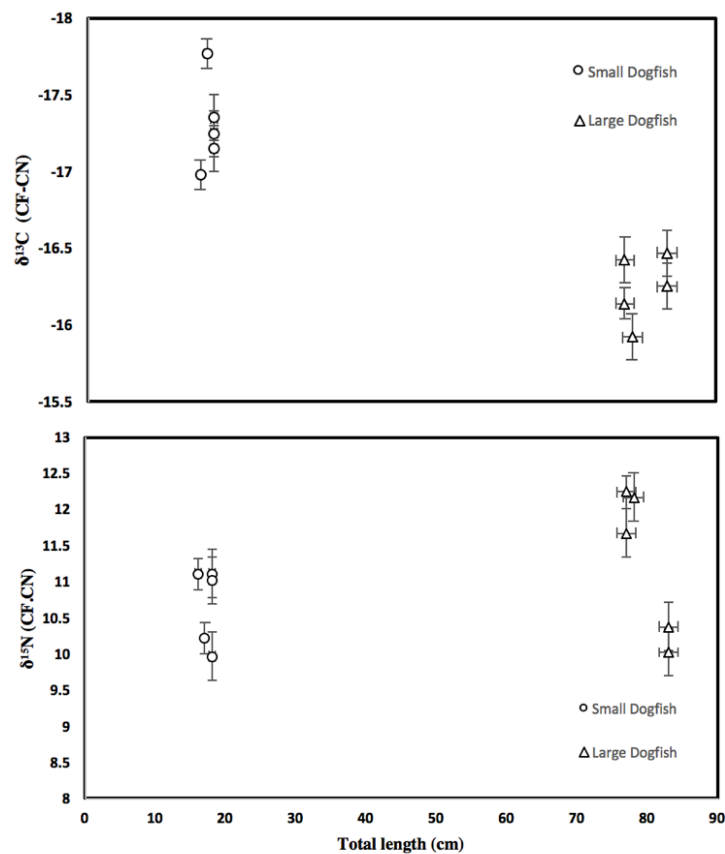


Figure 17 Mean $\delta^{13}\text{C} \pm$ SD (Top) and $\delta^{15}\text{N} \pm$ SD (bottom) measured in embryonic nucleus as a function of total length (cm).

3.3 Distribution

From 1991 to 2016, 7037 bottom trawl stations were distributed continuously from 67°N on the Greenland west coast to 65.9°N on the Greenland east coast (Figure 18). Seventy percent of these were trawled at depths shallower than 600m (N = 4889), while the remaining 30% were trawled at depths greater than 600m (N = 2062). Black dogfish were caught at 829 stations (11.8%, Table 4). Of the 5571 dogfish caught in this period, 89% (N = 4935) were measured (length, TL, cm) and sexed or noted as ‘unknown’ while the remaining 11% were weight. Most dogfish were caught in depths greater than 600 m (93%), while only 7% (N = 337) were caught shallower than 600m (Figure 19A).

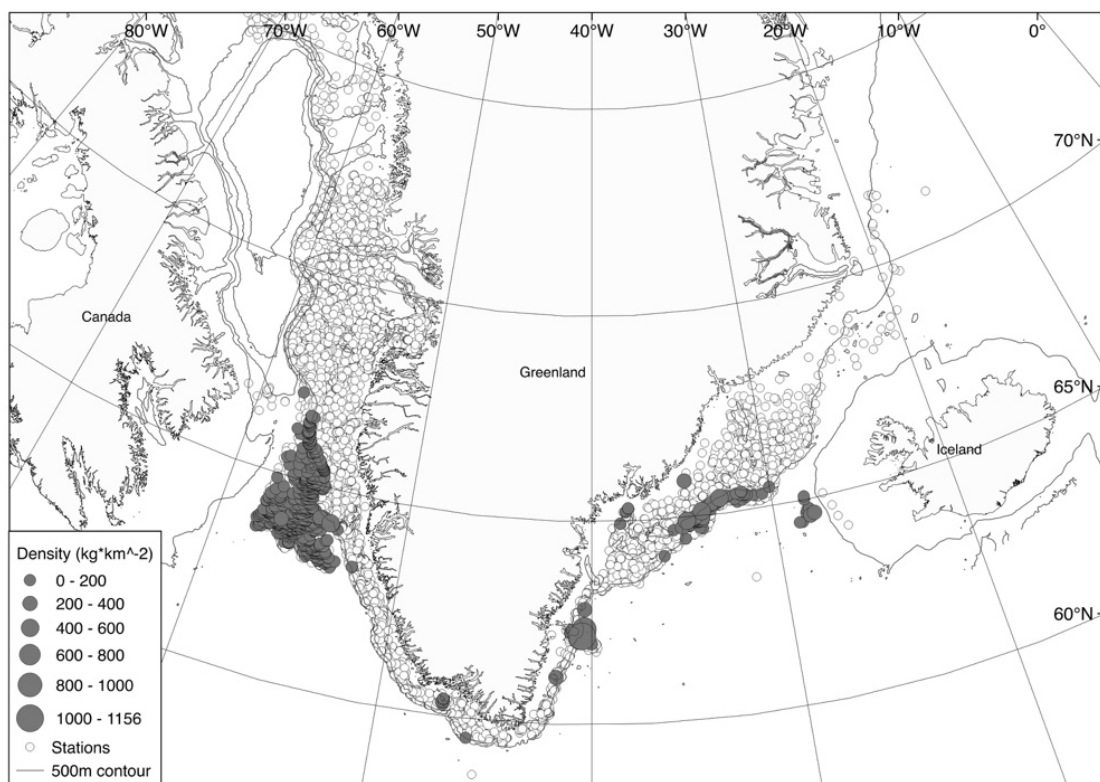


Figure 18 Distribution of black dogfish. Each empty circle represents a trawl station by Pamiut from 1991 to 2016 (N= 7037). Filled circles represents the density of sharks caught in the same time period (Average = 59.18 kg*km⁻², N= 5571).

Table 4 Distribution of black dogfish.

| | East | West | Min depth (m) | Max depth (m) | Min length (cm) | Max length (cm) |
|----------------|------|------|---------------|---------------|-----------------|-----------------|
| Females | 568 | 813 | 489 | 1493 | 16 | 90 |
| Males | 686 | 606 | 419 | 1481 | 16 | 82 |
| Unknown | 1432 | 830 | 328 | 1461 | 14 | 99 |
| Total | 2686 | 2249 | 328 | 1493 | 14 | 99 |

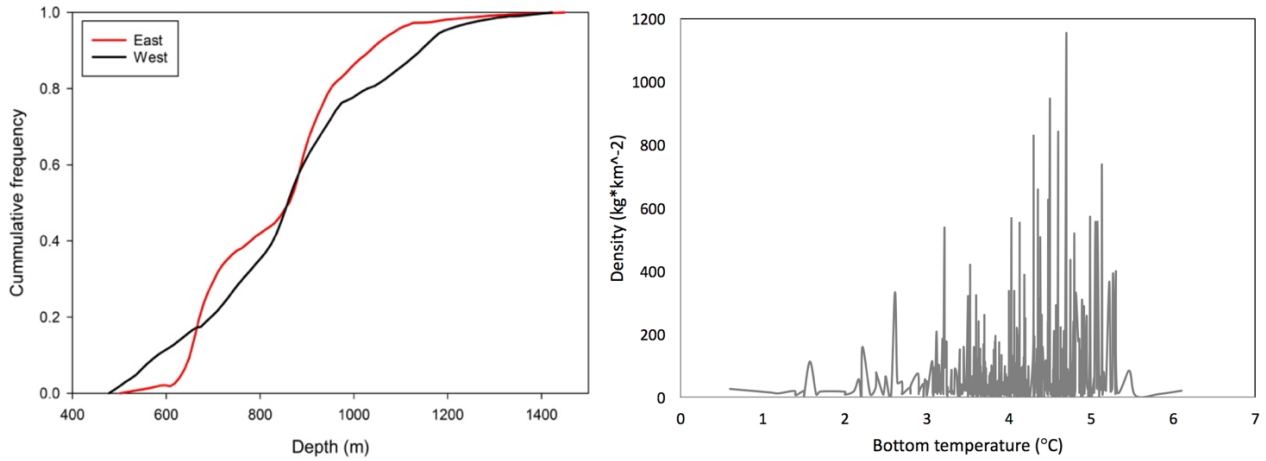


Figure 19 A: Occurrence by depth (m). 2249 black dogfish were caught in ‘West’, while 2686 were caught in ‘East’. B: Density of caught dogfish at different bottom temperatures.

There was a clear area related difference between ‘East’ and ‘West’. Nearly all black dogfish caught shallower than 600m originated from ‘West’ (N = 311, 92%, Figure 19A). Bottom water temperatures ranged from 0.6 to 6.1°C, with the majority of black dogfish caught between 4 and 5°C (Figure 19B).

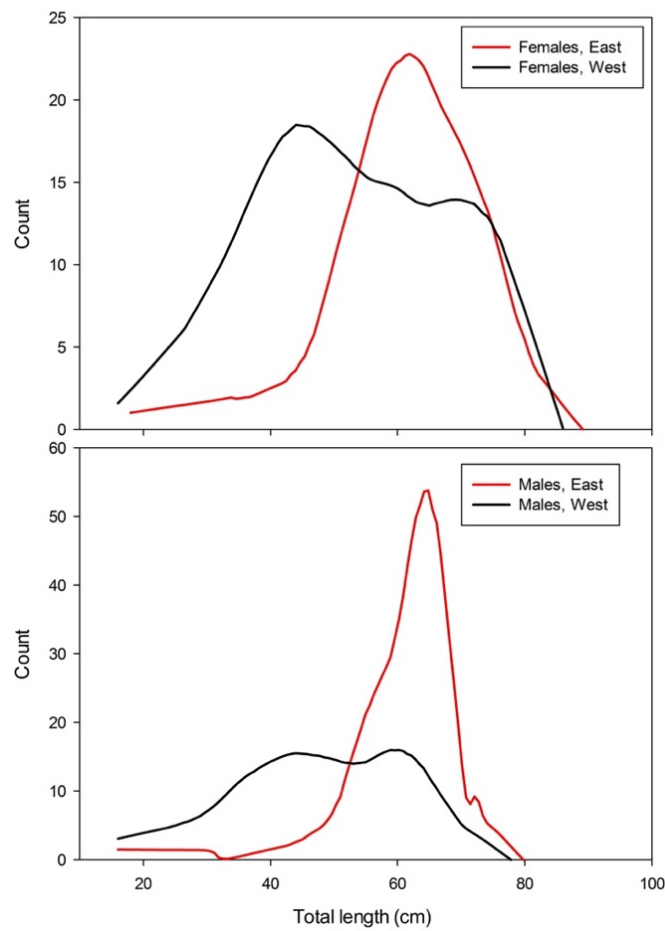


Figure 20 Length distribution for females (top) and males (bottom) in east (red) and west (black).

'West' area

The greatest occurrence of black dogfish caught in 'West' was between 63°N and 67°N (N = 2843, Figure 18). Within this area of high dogfish occurrence, black dogfish were caught in 87% (N = 3234) of the hauls, while it was only 35% (N = 8023) of hauls in the entire area. No black dogfish were caught north of 67°N, despite a trawling effort of 3703 stations at depths ranging from 26 to 1495m. From 60.4°N to 63°N dogfish were completely absent and south of 60.4°N catches were again few, with only 10 stations containing black dogfish. The capture depth for the entire western area ranged from 328 to 1493m, but most black dogfish were caught between 500 and 1100m (N = 2515, Figure 19A). Only 21 black dogfish were caught at depths less than 500m, while 334 black dogfish were caught deeper than 1100m.

In hauls containing dogfish, the average density was $31.15 \pm 45.38 \text{ kg*km}^{-2}$ (mean \pm SD). Both females and males were caught across the whole length span (Figure 20). Males were between 16 and 81cm (N= 606) with a mean length of 47.7cm. Females were between 16 and 86cm (N = 813) with an average length of 52.9cm. Females were significantly larger than males (ANOVA, Df = 1, F = 42.39, P<0.01).

'East' area

In 'East' the greatest occurrence of dogfish was between 62°N and 62.8°N (N = 1756), and 64°N and 65°N (N = 919) however they were absent in a large area (62.8°N to 64°N, Figure 18). In hauls containing dogfish the average density was $113.84 \pm 165.01 \text{ kg*km}^{-2}$. Dogfish were caught in 10% (N= 281) of all trawl hauls throughout this area (N= 2777), at depths between 402 and 1493m. Length distributions differed from the 'West' area. Smaller dogfish were rarely caught in this area, whereas larger dogfish were of similar size to individuals from 'West' (Figure 20). Males were between 16 and 82cm (N = 686) with an average length of 61.3cm. Females were between 18 and 90cm (N = 568) with an average length of 62.5cm. A significant difference in length was also found between sexes of this area, with females being larger than males (ANOVA, Df = 1, F = 6.467, P< 0.01).

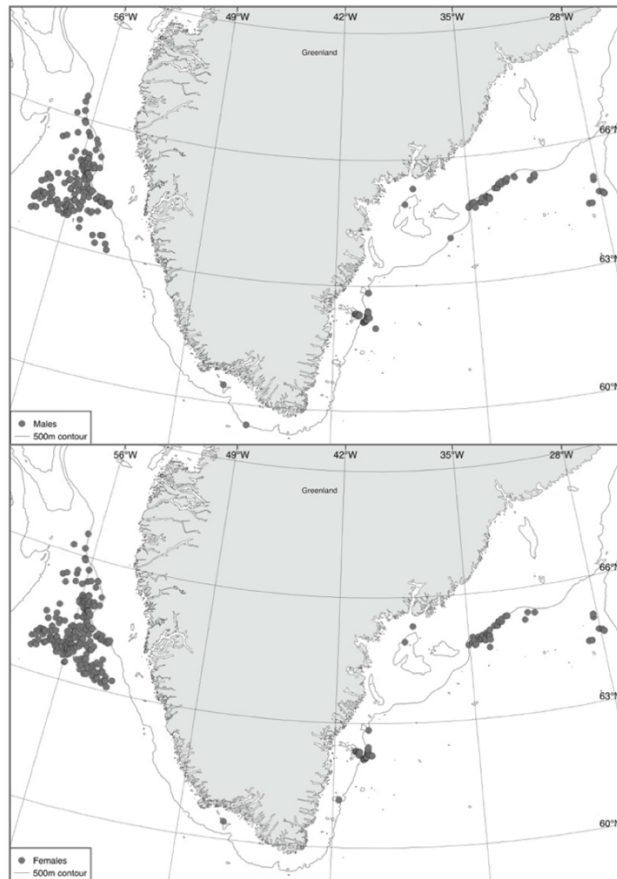


Figure 21 Distribution map for 1381 females (top) and 1292 males (bottom).

3.3.1 Biological information

Maps showing the distribution of females (N = 1381) and males (N = 1292) indicate a very high degree of overlap (Figure 21). Hence, there was no indication of any spatial separation by sex. Also no significant difference was found in the distribution of sex with depth (ANOVA, Df = 1, F = 0.074, P < 0.786). In general, individuals were larger at greater depths (Figure 22, P < 2e-16***). From the fitted regression, the average size increased 13.37cm for every 100m in depth. Also the temperature changes with the depth, but only 1°C for every 625m, making this rate much lower than the change in size.

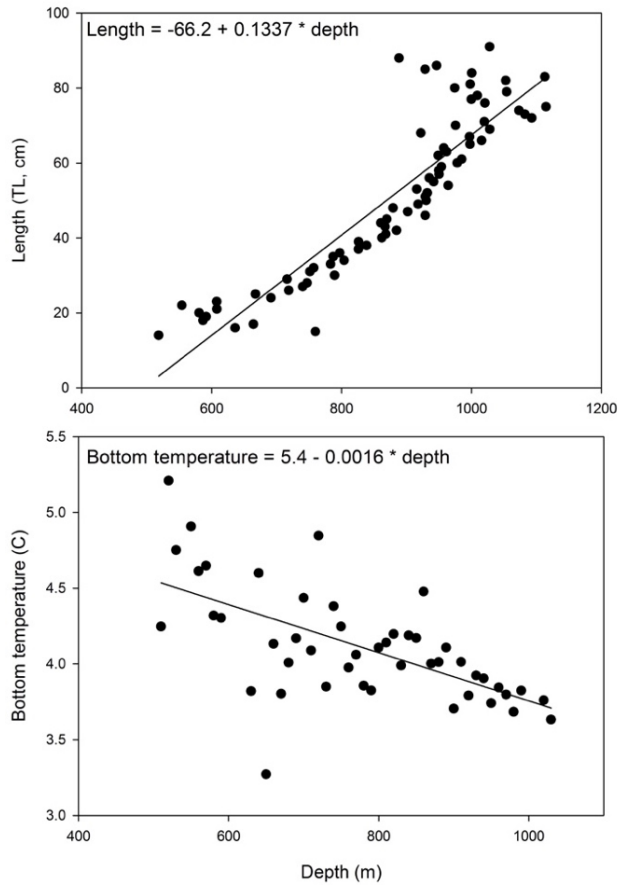


Figure 22 Length distribution throughout depths (m, top) and bottom temperature throughout depths (m, bottom).

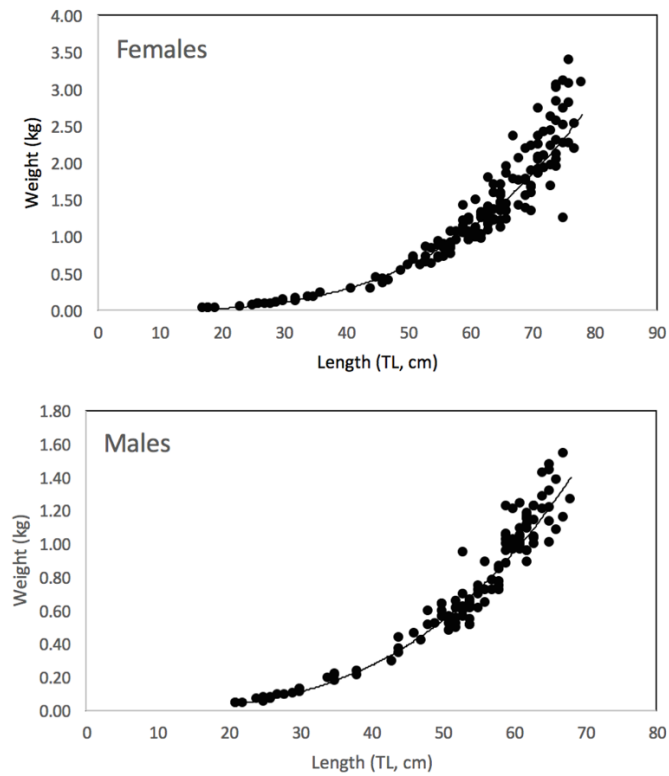


Figure 23 Length-weight relationship for females (top, N = 158) and males (bottom, N = 125).

The length-weight relationship for females (Figure 23) was best described as:

$$W = 0.1 \times 10^{-6} \times TL^{3.3052} \quad (P < 0.0001, R^2 = 0.98, TL: 17 \text{ to } 78 \text{ cm}, W: 0.02\text{-}3.6 \text{ kg})$$

and for males as:

$$W = 0.3 \times 10^{-6} \times TL^{3.092} \quad (P < 0.0001, R^2 = 0.98, TL: 18 \text{ to } 68 \text{ cm}, W: 0.02\text{-}1.5 \text{ kg})$$

These relationships show that both sexes have an allometric growth ($b \neq 3$), where the increase in weight is faster than the increase in length. The weight of females increases faster with increasing length than the weight of males. Furthermore, data show that females obtain a larger size than males.

3.4 Maturity

Females at all maturity stages were caught, whereof 6 were gravid, with most of them having developing embryos with external yolk-sacks (maturity-stage 4, Figure 24A and B), however, 2 females were carrying between 14 to 31 near-term embryos without external yolk-sack (maturity-stage 5, Figure 24C). Each near-term embryo weighed approximately 16 g and measured 16 cm (TL). It was observed that spines are developed in an early life stage (Figure 24B). Females become sexually mature at a length of 65cm (Figure 25), corresponding to 72% of their maximum size and ~27 years of age. Males however, become sexually mature at a length of 43cm (Figure 25) which is equivalent to 52% of their maximum size and ~15 years of age.

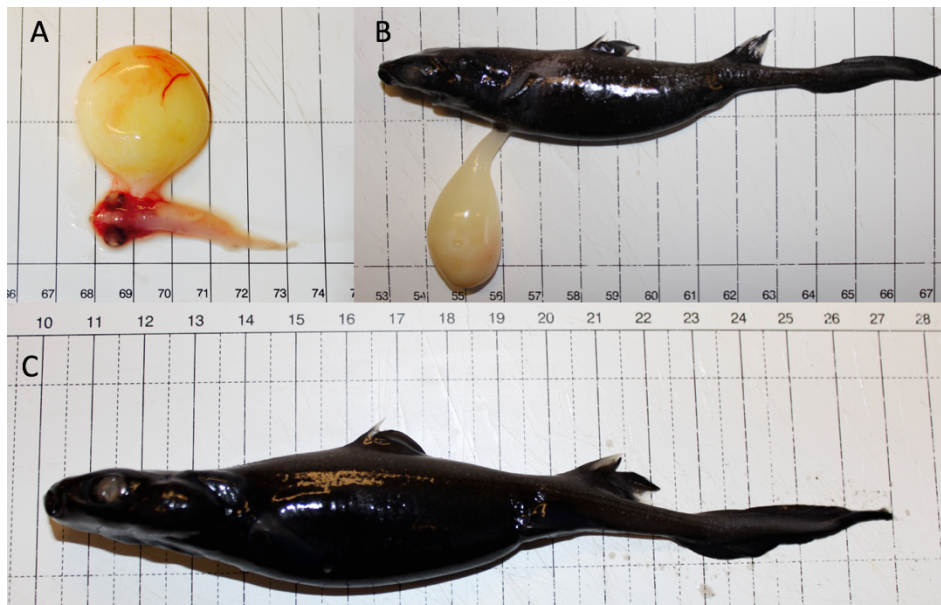


Figure 24 Embryo stages. A: Embryo with yolk-sack (early stage 4), B: Embryo with yolk-sack (late stage 4) and C: Embryo without yolk-sack (stage 5).

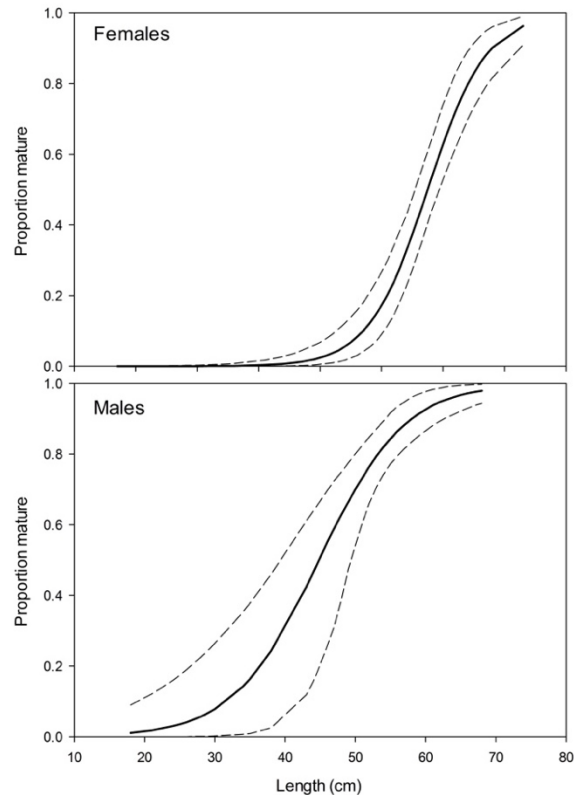


Figure 25 Maturity ogives for females (top) and males (bottom) shown with 95% confidence intervals in black dogfish.

4 Discussion

4.1 Age estimation and validation

Although age estimates of dogfish often have been based on visible bands growing externally on the spine (Beamish and McFarlane, 1985, Campana et al., 2006), this was not possible for black dogfish. The bands were either too poorly defined for age estimation or missing altogether (Figure 8). Similar observations were described in studies of the needle dogfish (*C. acus*, Tanaka 1990) and the leafscale gulper shark (*C. squamosus*, Clarke et al., 2002). Nor did heat treatment make the surface structures more visible (Figure 5), indicating that a well-known method may not work in all species, possibly due to differences in spine structure. Longitudinal sections of spines revealed structures, but based on the growth of the spine, these were probably not laid down annually (Figure 3B and 6). This method was therefore proved unfitting for age estimation. As a result, cross-sections revealed the only opportunity to expose internal growth bands and thereby estimating the age of black dogfish from spines.

Soldat (1982) describe that spiny dogfish grow embryonically for about two years before they are born. Furthermore, readings of cross-sections proposed that the first growth band was laid down before birth

(Soldat, 1982; Tanaka, 1990). This growth band is known as an "embryonic annual ring"(Soldat, 1982). However, timespan for embryonic growth in black dogfish is unknown, thus further investigation is necessary. Still, results showed full-term embryos with dorsal fin spines (Figure 24), suggesting that these were formed during embryonic development. Additionally, cross-sections of these embryonic spines revealed an annual ring (Figure 11). Embryonic annual rings were counted as the first growth band, which meant that all dogfish, counted at least one year of age.

According to previous studies, a maximum count of growth bands was observed proximal to the constriction of the internal pulp cavity (Clarke et al., 2001; Beamish and McFarlane, 1985). However, for black dogfish this specific cross-section was frequently vague and instead sections obtained distal to the constriction of the internal pulp cavity was used (Figure 9). Cross-sections were chosen based on visibility of growth bands, however, the clearest cross-section did not always contain a maximum number of growth bands of the spine, suggesting that low visibility could cause an uncertainty for age estimation, even though a standardized method was obtained. Growth bands were located internally in the stem of the spine, but instead of cross-sections with a clear division of inner, middle and outer dentine, as described in the spines of the spiny dogfish, these had a somewhat homogenous appearance throughout whole sections (Figure 10). However, a lack of spines from the spiny dogfish makes it impossible to determine whether or this is a coincidence or varies like the ones of the black dogfish. A low percentage of CV was reported in this study (Figure 14 and 15), indicating a high level of reproducibility and precision of growth band readings in spines. As counting was performed without knowledge of the other readers' band-counts or the length of the specimen, this was notable and suggested that cross-sections were easy to read. A high precision however, cannot tell anything about the accuracy of the method.

Readings of cross-sections from the spine of the spiny dogfish showed an age estimate of approximately 17 years (Figure 10D). These results corresponded well with the VBGF for this species (Figure 2) suggesting that the method of band readings in cross-sections could be usable for age estimations.

Cross-sections of spines provided maximum age estimates of 38 years for females and 37 years for males (Figure 12, Appendix I). Radiocarbon analysis however, demonstrated that five of the largest black dogfish had lens nuclei with a low pMC value, indicating that this tissue was formed in the pre-bomb period (Figure 16). According to Scourse et al. (2012) the ^{14}C amounts almost doubled in the atmosphere in the early 1960's and the bomb pulse was created and became detectable in the marine environment, across the northern North Atlantic, not later than the mid 1960' (Figure 4). Hence, this

suggest that the largest dogfish in this study was a minimum of 50 years old. Ages estimated from the VBGF however, suggest that these were not older than between 38 and 47 years (Table 3). Radiocarbon analyses therefore indicate that age estimations provided by growth readings based on cross-sections of spines are underestimating the age of the black dogfish, at least for the largest individuals. To investigate whether or not radiocarbon analyses provided a valid estimation of age, it is important to understand the transportation of radiocarbon down through the water column. Williams et al. (1987) proposed that radiocarbon is incorporated as dietary carbon into food webs and through these food webs, radiocarbon was rapidly transported down through the water column to the bathypelagic zone (3000 m) from its origin in the epipelagic zone. Despite the fact that black dogfish as a deep water species, live in the meso- and bathypelagic deep waters, the rapid transport suggested that incorporation of radiocarbon into the body of black dogfish, happened without any time lag. $\delta^{13}\text{C}$ values of embryonic nuclei averaged $-16.77 \pm 0.14\%$. Results showed an increased depletion of the lens nuclei from the small dogfish (Figure 17), which may be caused by several processes. One could be that the diet may have changed over time (Christensen and Richardson, 2008). However, similar $\delta^{15}\text{N}$ values between all embryonic nuclei suggest that the trophic position have not changed over time, coincide with no structural changes in food web structure over time. Another explanation could be that the $\delta^{13}\text{C}$ values may differ between areas, as large and small dogfish originated from the areas East and West, respectively (Table 3). Differences in $\delta^{13}\text{C}$ values between areas have been discovered earlier for both Atlantic cod (*Gadus morhua*) and the Greenland halibut (*Reinhardtius hippoglossoides*) (Hansen et al., 2012) suggesting that the value of $\delta^{13}\text{C}$ most likely is area specific. Stable isotopes analysis resulted in relative high values of $\delta^{15}\text{N}$ (Figure 17), indicating a high trophic position, consistent with analyses of stomach content (Qvist, unpublished data) showing that fish is the main prey item.

These results suggest that radiocarbon analysis most likely provide a valid method for age estimating the black dogfish. Unfortunately, only a limited number of samples were analyzed, making it impossible to determine the exact timing of incorporation of radiocarbon and the length of black dogfish at the peak of the bomb pulse (Figure 4, Williams 1987; Scourse et al., 2012, Nielsen et al., 2016). Further validation of age and growth rates can be accomplished from comparison between a growth rate derived from a more thorough radiocarbon analysis of eye lenses and a growth rate derived from radiocarbon analysis based on date-specific incorporation of ^{14}C in the dorsal fin spines.

Underestimation occurs in especially older individuals, possibly after the onset of sexual maturity (Francis et al., 2007; Harry, 2017). A correlation between dogfish length and both spine length and spine width showed a strong linear relationship (Figure 13). This relationship could indicate that an

underestimation would be explained by ceasing of spine growth after maturation, due to allocation of energy to reproduction (Francis et al., 2007; Harry, 2017). However, nothing suggests that spines cease to grow, why an underestimation of age might instead be explained due to deposition of vanishingly-narrow increments, breakage and wearing of fin spines or the fact that growth bands might not be deposited annually. Because of their bathymetric distribution (Figure 18A) black dogfish live a part of their life in complete darkness, cold temperatures, and under high hydrostatic pressure. Complete darkness and constant cold temperatures creates a constant environment (Treberg and Speers-Roesch, 2016), making it impossible to distinguish between seasons and thus possible that growth bands might not be deposited annually but based on food consumption. However, this needs to be examined further.

Growth parameters show that females grow with a growth rate less steep than males, suggesting that males reach their theoretical maximum length quicker than females (Figure 12, Table 2). Furthermore, a sexual dimorphism, with females being larger than males, was recorded, while females weight increases faster with increasing length than males' (Figure 23) as reported earlier by Yano (1995). The greater size achieved by females is common in most elasmobranchs species (Yano, 1995; Cortés, 2000; Gennari and Scacco, 2007). A study by Gennari and Scacco (2007) suggested that these differences in theoretical maximum length between sexes are due to a delayed female maturation in comparison to males. When reaching maturity, allocation of energy shifts and the rate at which growth occurs would decline, making males grow slower than females. Maturity ogives presented in this study confirms this delay as females mature 12 years later than males (Figure 25). Females mature at a length corresponding to 72% of their maximum length, which was consistent with the assumption that fish and sharks generally mature at lengths corresponding to 65-80 % of their maximum length (Beverton and Holt, 1959). A large size at maturity is favorable, since reproductive output increases with size (Jennings et al., 2009).

This was the first known study investigating the use of spines for providing age and growth parameters for black dogfish in the Greenland waters. No validation has been obtained for this method and therefore there is no consensus of how to estimate the age of black dogfish. However, results suggest that black dogfish despite its small size is actually long lived (Table 2).

Supplementary studies are needed before a validated method for determination of age of this species can be obtained. According to Buble et al. (2012) vertebral centra provides a more exact mean for estimating the age of spiny dogfish, than spines. Vertebral centra differ from spines by growing internally and not being subject to environmental wear or breakage. Therefore, by utilizing an ageing structure such as the vertebral centrum, the sources of error may be eliminated, which ultimately leads

to increased precision and accuracy of age estimates compared to age estimates derived from spines. However, Francis et al. (2007) strongly suggest that the vertebrae of some old, long-lived shark species either deposit vanishingly-narrow increments, or cease to grow altogether, after a certain age, resulting in an underestimation of age as with the spines. The use of radiocarbon analysis based on spines has shown to be well suited as an age validation method for the spiny dogfish, a close relative to the black dogfish (Campana et al., 2006). Also mark–recapture analysis with oxytetracycline (OTC) has proven useful as an age validation method (Beamish and McFarlane, 1985; McFarlane and Beamish, 1987; Matta et al., 2017), but this requires a substantial number of recaptures, which is unlikely for a non-commercial species like black dogfish. The best hope of validating age is therefore to make a comprehensive radiocarbon analysis of eye lens nuclei for all sizes of the black dogfish.

4.3 Distribution

The extensive trawl data used in this study provides a good outline of the distribution patterns of black dogfish in Greenland waters on a large scale. A northern limit for the distribution was found in both areas (Figure 18). The water masses around Greenland are complex, with the West Greenland Current consisting of the saline temperate Irminger Current, from the Atlantic Ocean and the cold low-saline East Greenland Current originating from the Arctic Ocean (Hansen et al., 2012; Ribergaard, 2014). The complexity and gradual mixing of the different water masses as they flow north towards the Polar Waters, results in dilution and branching of the main part of the West Greenland Current westward to the Labrador Current (Ribergaard, 2014). The branching of the warmer West Greenland Current towards the north could be a plausible explanation for the distribution of the black dogfish as they prefer temperatures about 4-5°C and disappear at temperatures below 1 °C (Figure 19B). East of Greenland the East Greenland Current mix with the Polar Waters even further south than in the west, suggesting that the limiting factor of the distribution are most likely temperature.

The depth preferences of black dogfish (Figure 19A) show a high overlap to the primary trawling depths of the Greenland halibut (800-1400m, Jorgensen et al., 2014), indicating that this fishery pose a threat to the black dogfish population and that it is vulnerable as a bycatch species. Furthermore, Jorgensen et al. (2014), reported a significant negative cross-correlation between individual mean weight and effort in black dogfish. Mean weight of black dogfish decreased 26%, indicating a shift in length composition to smaller sizes due to size-selective properties of the used gear in the commercial fishery for Greenland halibut.

No significant difference was found in the bathymetric distribution between sexes, even though females were caught at greater depths than males (Table 4). However, depth had a significant effect on the size of black dogfish (Figure 22) showing that dogfish length increased with increasing depth. These results suggest a ‘bigger-deeper’ phenomenon, which has been previously described for black dogfish in West Greenland waters by Yano (1995). This phenomenon is thought to be applicable to many deep-water species, however it was not found in a study by Jakobsdóttir (2001), suggesting that it could vary between geographical areas.

Nothing indicated that females and males occupied different areas (Figure 21) however, smaller dogfish were rarely caught in the East (Figure 20). An explanation could be that pregnant females migrate to the areas in West when pupping. Such migration was reported for black dogfish in the Canadian waters, where pregnant females migrate to shallow depths of the Laurentian Channel when pupping (Kulka, 2006). However, this should be investigated further.

5 Conclusion

Using fin spine growth bands, I have provided the first age estimates for black dogfish. Based on radiocarbon dating, these estimates are however minimum estimates as the largest individuals appear to be more than 50 years old. The reason for this underestimation is unknown, but continued spine growth with length suggest it is linked with non-annual growth band deposition at older ages or vanishing-narrow growth bands in the layers of the fin spine. Additional studies using more lengths for radiocarbon dating could shed further light on the accuracy of the age readings as could tagging studies.

The data on trawl catches clearly show the distributional limit of black dogfish in both East and West Greenland. These are well connected with the dominating current system around Greenland and the temperature preferences of black dogfish. Moreover, the depth preferences are clearly shown and illustrate that the black dogfish is vulnerable as a bycatch species in bottom trawl fisheries; especially those targeting Greenland halibut.

References

- Bassnett, S., Shi, Y., & Vrensen, G. F. (2011). Biological glass: structural determinants of eye lens transparency. *Philosophical Transactions of the Royal Society of London B: Biological Sciences*, **366**(1568), 1250-1264.
- Beamish, R. J., & McFarlane, G. A. (1985). Annulus development on the second dorsal spine of the spiny dogfish (*Squalus acanthias*) and its validity for age determination. *Canadian Journal of Fisheries and Aquatic Sciences*, **42**(11), 1799-1805.
- Beverton, R. J. H., Holt, S. J. (1957). On the dynamics of exploited fish populations. Fish Invest MAFF GB, 2 *Sea Fish* **19**: 533.
- Beverton, R. J. H., Holt, S. J. (1959). A review of the lifespan and mortality rates of fish in nature and their relationship to growth and other physiological characteristics. *Ciba Foundation Colloquium on Ageing* **5**: 142- 180.
- Bowman, S. (1990). Interpreting the past, Radiocarbon. British Museum and the University of California: 9-49.
- Bubley, W. J., Kneebone, J., Sulikowski, J. A. & Tsang, P. C. (2012). Reassessment of spiny dogfish *Squalus acanthias* age and growth using vertebrae and dorsal-fin spines. *J Fish Biol* **80**(5), 1300-1319.
- Cailliet, G. M. (1990). Elasmobranch age determination and verification: an updated review. *NOAA Tech. Rep. NMFS* **90**, 157-165.
- Campana, S. E. (2001). Accuracy, precision and quality control in age determination, including a review of the use and abuse of age validation methods. *Journal of fish biology*, **59**(2), 197-242.
- Campana, S. E., & Thorrold, S. R. (2001). Otoliths, increments, and elements: keys to a comprehensive understanding of fish populations?. *Canadian Journal of Fisheries and Aquatic Sciences*, **58**(1), 30-38.
- Campana, S. E., Natanson, L. J. & Myklevoll, S. (2002). Bomb dating and age determination of large pelagic sharks. *Canadian Journal of Fisheries and Aquatic Sciences* **59**(3), 450-455.
- Campana, S. E., Jones, C., McFarlane, G. A. & Myklevoll, S. (2006). Bomb dating and age validation using the spine of spiny dogfish (*Squalus acanthias*). *Environmental Biology of Fishes* **77**, 327-336.
- Christensen, J. T., & Richardson, K. (2008). Stable isotope evidence of long-term changes in the North Sea food web structure. *Marine Ecology Progress Series*, **368**, 1-8.
- Claes, J. M., Nilsson, D. E., Straube, N., Collin, S. P. & Mallefet, J. (2014). Iso-luminance counterillumination drove bioluminescent shark radiation. *Scientific Reports* **4**, srep04328.
- Clarke, M. W., Connolly, P. L. & Bracken, J. J. (2001). Aspects of reproduction of the deep water shark *Centroscymnus coelolepis* and *Centrophorus squamosus* from west of Ireland and Scotland. *Journal of the Marine Biological Association of the United Kingdom* **81**(6), 1019-1029.

- Clarke, M. W., Connolly, P. L., & Bracken, J. J. (2002). Age estimation of the exploited deepwater shark *Centrophorus squamosus* from the continental slopes of the Rockall Trough and Porcupine Bank. *Journal of Fish Biology*, **60**(3), 501-514.
- Clarke, M. W. & Irvine, S. B. (2006). Terminology for the ageing of chondrichthyan fish using dorsal-fin spines. *Environmental Biology of Fishes* **77**(3-4), 273-277.
- Cohen, A. I. (1965). The electron microscopy of the normal human lens. *Investigative Ophthalmology & Visual Science*, **4**(4), 433-446.
- Compagno, L.J.V. (1984). FAO Species Catalogue. Vol. 4. Sharks of the World. An annotated and illustrated catalogue of shark species known to date. Part 1. Hexanchiformes to Lamniformes. *FAO Fish. Synop.*, (125) **4**:47-48.
- Cortés, E. (2000). Life history patterns and correlations in sharks. *Rev Fish Sci* **8**(4):299–344.
- Cotton, C. F., Andrews, A. H., Cailliet, G. M., Grubbs, R. D., Irvine, S. B. & Musick, J. A. (2014). Assessment of radiometric dating for age validation of deep-water dogfish (Order: Squaliformes) finspines. *Fisheries Research* **151**, 107-113.
- Ebert, D.A., Crozier, P. & Blasdale, T. & McCormack, C. 2009. *Centroscyllium fabricii*. *The IUCN Red List of Threatened Species 2009*: e.T161521A5442458.
<http://dx.doi.org/10.2305/IUCN.UK.2009-2.RLTS.T161521A5442458.en>
- Fabens, A. J. (1965). Properties and fitting of the von Bertalanffy growth curve. *Growth*, **29**, 265-289.
- Francis, M. P., Campana, S. E., & Jones, C. M. (2007). Age under-estimation in New Zealand porbeagle sharks (*Lamna nasus*): is there an upper limit to ages that can be determined from shark vertebrae?. *Marine and Freshwater Research*, **58**(1), 10-23.
- Fuiman, L. A., & Werner, R. G. (Eds.). (2009). *Fishery science: the unique contributions of early life stages*. John Wiley & Sons, 64-79.
- Gennari, E., & Scacco, U. (2007). First age and growth estimates in the deep water shark, *Etmopterus spinax* (Linnaeus, 1758), by deep coned vertebral analysis. *Marine Biology*, **152**(5), 1207-1214.
- Goldman, K. J., Cailliet, G. M., Andrews, A. H., & Natanson, L. J. (2012). Assessing the age and growth of chondrichthyan fishes. *Biology of Sharks and their Relatives*, **13**, 423, chapter 14.
- Gordon, J. D. M. & Duncan, J. A. R. (1985). The Ecology of the Deep-Sea Benthic and Benthopelagic Fish on the Slopes of the Rockall Trough, Northeastern Atlantic. *Progress in Oceanography* **15**(1), 37-69.
- Hamady, L. L., Natanson, L. J., Skomal, G. B., & Thorrold, S. R. (2014). Vertebral bomb radiocarbon suggests extreme longevity in white sharks. *PloS one*, **9**(1), e84006.
- Hansen, J. H., Hedeholm, R. B., Sünksen, K., Christensen, J. T., & Grønkjær, P. (2012). Spatial variability of carbon ($\delta^{13}\text{C}$) and nitrogen ($\delta^{15}\text{N}$) stable isotope ratios in an Arctic marine food web. *Marine Ecology Progress Series*, **467**, 47-59.

- Harry, A. V. (2017). Evidence for systemic age underestimation in shark and ray ageing studies. *Fish and Fisheries*.
- Heessen, H. J. L. (2004). ICES Fish-Map: mapping North Sea fish. *ICES newsletter*.
- Jakobsdottir, K. B. (2001). Biological aspects of two deep-water squalid sharks: *Centroscyllium fabricii* (Reinhardt, 1825) and *Etmopterus princeps* (Collett, 1904) in Icelandic waters. *Fisheries Research* **51**(2), 247-265.
- Jennings, S., Kaiser, M., & Reynolds, J. D. (2009). Marine fisheries ecology. *John Wiley & Sons*, 56-270.
- Jorgensen, O. A., Bastardie, F. & Eigaard, O. R. (2014). Impact of deep-sea fishery for Greenland halibut (*Reinhardtius hippoglossoides*) on non-commercial fish species off West Greenland. *ICES Journal of Marine Science* **71**(4), 845-852.
- Kalish, J. M. (1993). Pre- and post-bomb radiocarbon in fish otoliths. *Earth and Planetary Science Letters* **114**(4): 549-554.
- Kerr, L. A., Andrews, A. H., Cailliet, G. M., Brown, T. A., & Coale, K. H. (2006). Investigations of $\Delta 14C$, $\delta 13C$, and $\delta 15N$ in vertebrae of white shark (*Carcharodon carcharias*) from the eastern North Pacific Ocean. *Environmental Biology of Fishes*, **77**(3-4), 337-353.
- Kulka, D. W. Serial No. N5237 NAFO SCR Doc. 06/20 SCIENTIFIC COUNCIL MEETING–JUNE 2006.
- Libby, W. F. (1960). Radiocarbon dating. Nobel Lecture, December 12.
- Matta, M. E., Tribuzio, C. A., Ebert, D. A., Goldman, K. J., & Gburski, C. M. (2017). Age and growth of elasmobranchs and applications to fisheries management and conservation in the Northeast Pacific Ocean. In *Advances in Marine Biology* (Vol. 77, pp. 179-220). Academic Press.
- McFarlane, G. A., & Beamish, R. J. (1987). Validation of the dorsal spine method of age determination for spiny dogfish. *Age and Growth of Fish*. *Iowa State University Press, Ames, Iowa*, 287-300.
- McPhie, R. P. & Campana, S. E. (2009). Bomb dating and age determination of skates (family Rajidae) off the eastern coast of Canada. *ICES Journal of Marine Science* **66**(3): 546-560
- Mendoza, R. R. (2006). Otoliths and their applications in fishery science. *Ribarstvo*, **64**(3), 89-102.
- Menni, R. C., Burgess, G. H., & García, M. L. (1990). Occurrence of *Centroscyllium fabricii* Reinhardt, 1825) Elasmobranchii, Squalidae in the Beagle Channel, southern South America. In *Gilbert L. Voss Int. Symp. Held at the American Malacological Union Annu. Meet. Woods Hole, MA, USA. 3-7 June 1990*.
- Nielsen, J., (2013). Master thesis: Age estimation and feeding ecology of Greenland shark *Somniosus microcephalus* in Greenland waters. University of Copenhagen, 1-81.

Nielsen, J., Hedeholm, R. B., Heinemeier, J., Bushnell, P. G., Christiansen, J. S., Olsen, J., Ramsey, C. B., Brill, R. W., Simon, M., Steffensen, K. F. & Steffensen, J. F. (2016). Eye lens radiocarbon reveals centuries of longevity in the Greenland shark (*Somniosus microcephalus*). *Science* **353**(6300), 702-704.

Ogle, D. H., & Isermann, D. A. (2017). Estimating Age at a Specified Length from the von Bertalanffy Growth Function. *North American Journal of Fisheries Management*, **37**(5), 1176-1180.

Post, D. M. (2002). Using stable isotopes to estimate trophic position: models, methods, and assumptions. *Ecology*, **83**(3), 703-718.

Qvist, T. (2017). Feeding ecology of the Black dogfish (*Centroscyllium fabricii*). In preparation.

Ribergaard, M. H., & Buch, E. (2008). Oceanographic investigations off west Greenland 2007. *NAFO Scientific Council Documents*, **7**(003).

Scourse., J. D., Wanamaker, A. D., Weidman, C., Heinemeier, J., Reimer, P. J., Butler, P. G., Witbaard, R. & Richardson, C. A. (2012). The marine radiocarbon bomb pulse across the temperate North Atlantic; a compilation of $\Delta 14C$ time histories from *Arctica islandica* growth increments. *Radiocarbon* **54**(2): 165-186.

Soldat, V. T. (1982). Age and size of spiny dogfish, *Squalus acanthias*, in the northwest Atlantic. *North Atlantic Fisheries Organisation Scientific Council Studies* **3**, 47-52.

Stevens, J. D., Bonfil, R., Dulvy, N. K., & Walker, P. A. (2000). The effects of fishing on sharks, rays, and chimaeras (chondrichthyans), and the implications for marine ecosystems. *ICES Journal of Marine Science*, **57**(3), 476-494.

Stuvier M, Polach HA (1977). Reporting of C-14 data-discussion. *Radiocarbon* **19**(3): 355-363.

Tanaka, S. (1990). The Structure of the Dorsal Spine of the Deep-Sea Squaloid Shark *Centrophorus-Acus* and Its Utility for Age-Determination. *Nippon Suisan Gakkaishi* **56**(6), 903-909.

Taylor, V. L., Al-Ghoul, K. J., Lane, C. W., Davis, V. A., Kuszak, J. R., & Costello, M. J. (1996). Morphology of the normal human lens. *Investigative ophthalmology & visual science*, **37**(7), 1396-1410.

Taylor, I. G., Gertseva, V. & Matson, S. E. (2013). Spine-based ageing methods in the spiny dogfish shark, *Squalus suckleyi*: How they measure up. *Fisheries Research* **147**, 83-92.

Treberg, J. R., & Speers-Roesch, B. (2016). Does the physiology of chondrichthyan fishes constrain their distribution in the deep sea?. *Journal of Experimental Biology*, **219**(5), 615-625.

Van der Merwe, N. J. (1982). Carbon Isotopes, Photosynthesis, and Archaeology: Different pathways of photosynthesis cause characteristic changes in carbon isotope ratios that make possible the study of prehistoric human diets. *American Scientist*, **70**(6), 596-606.

Von Bertalanffy, L. (1938). A quantitative theory of organic growth (inquiries on growth laws II). *Human Biol.*, **10**(2): 181-213.

- Walker, T. I., Taylor, B. L., Hudson, R. J., & Cottier, J. P. (1998). The phenomenon of apparent change of growth rate in gummy shark (*Mustelus antarcticus*) harvested off southern Australia. *Fisheries Research*, **39**(2), 139-163.
- Williams, P. M., Druffel, E. R. M., & Smith, K. L. (1987). Dietary carbon sources for deep-sea organisms as inferred from their organic radiocarbon activities. *Deep Sea Research Part A. Oceanographic Research Papers*, **34**(2), 253-266.
- Wootton, R. J. (2012). Ecology of teleost fishes (Vol. 1). *Springer Science & Business Media*, 63-130.
- Yano, K. (1995). Reproductive biology of the black dogfish, *Centroscyllium fabricii*, collected from waters off western Greenland. *Journal of the Marine Biological Association of the United Kingdom* **75**(2), 285-310.
- Yano, K. & Tanaka, S. (1984). Some biological aspects of the deep sea Squaloid shark *Centroscymnus* from Suruga Bay, Japan. *Bulletin of the Japanese Society of Scientific Fisheries* **50**(2), 249–256.
- Yigin, C. C. & Ismen, A. (2016). Age and Growth of Spiny Dogfish *Squalus acanthias* (Squalidae: Chondrichthyes) in the North Aegean Sea. *Pakistan Journal of Zoology* **48**(4), 1185-1191.
- Young, R. E. (1983). Oceanic Bioluminescence: an Overview of General Functions. *Bulletin of Marine Science* **33**(4), 829-845.

Appendix I

Table 1 Summary of all age estimated black dogfish.

| Area | Dogfish ID | Sex | Total length (cm) | Total weight (kg) | Age count |
|------|------------|-----|-------------------|-------------------|-----------|
| W | 21 | M | 59 | 1054 | 27 |
| W | 22 | F | 55 | 932 | 18 |
| W | 38 | F | 54 | 624 | 24 |
| W | 39 | M | 59 | 1018 | 30 |
| W | 40 | F | 51 | 684 | 20 |
| W | 46 | F | 41 | 298 | 15 |
| W | 52 | F | 70 | 1884 | 31 |
| W | 56 | M | 54 | 664 | 24 |
| W | 57 | M | 44 | 370 | 37 |
| W | 58 | M | 53 | 698 | 21 |
| W | 76 | F | 73 | 2224 | 25 |
| W | 158 | F | 66 | 1334 | 25 |
| W | 171 | M | 26 | 74 | 7 |
| W | 174 | F | 26 | 74 | 6 |
| W | 178 | F | 26 | 74 | 1 |
| W | 180 | F | 26 | 86 | 1 |
| W | 184 | M | 25 | 72 | 1 |
| W | 190 | M | 22 | 40 | 1 |
| W | 192 | M | 21 | 42 | 4 |
| W | 193 | F | 26 | 82 | 6 |
| W | 196 | M | 26 | 64 | 7 |
| W | 200 | F | 18 | 20 | 1 |
| W | 203 | M | 24 | 62 | 7 |
| W | 206 | M | 21 | 36 | 4 |
| W | 207 | M | 18 | 18 | 2 |
| W | 210 | F | 23 | 50 | 4 |
| W | 211 | F | 19 | 28 | 1 |
| W | 233 | M | 61 | 1042 | 23 |
| W | 238 | M | 52 | 612 | 18 |
| W | 240 | F | 51 | 718 | 16 |
| W | 274 | M | 58 | 844 | 32 |
| W | 276 | M | 43 | 290 | 19 |
| W | 283 | F | 74 | 2110 | 33 |
| E | 3 | F | 56 | 828 | 21 |
| E | 8 | F | 53 | 846 | 21 |
| E | 9 | F | 71 | 1910 | 28 |
| E | 13 | M | 66 | 1382 | 31 |
| E | 14 | M | 67 | 1544 | 36 |
| E | 15 | F | 61 | 1124 | 22 |
| E | 25 | F | 77 | 2524 | 38 |
| E | 30 | M | 62 | 1116 | 32 |

| | | | | | |
|---|-----|---|----|------|----|
| E | 32 | M | 65 | 1472 | 20 |
| E | 34 | M | 62 | 1164 | 25 |
| E | 61 | F | 65 | 1542 | 24 |
| E | 66 | F | 59 | 1044 | 17 |
| E | 79 | M | 50 | 634 | 17 |
| E | 81 | M | 53 | 946 | 17 |
| E | 85 | F | 60 | 1202 | 26 |
| E | 93 | M | 53 | 622 | 24 |
| E | 95 | M | 49 | 520 | 23 |
| E | 96 | M | 55 | 720 | 26 |
| E | 99 | M | 55 | 746 | 16 |
| E | 100 | F | 45 | 432 | 15 |
| E | 101 | M | 54 | 652 | 22 |
| E | 107 | M | 56 | 640 | 24 |
| E | 112 | F | 61 | 1070 | 27 |
| E | 113 | F | 58 | 956 | 25 |
| E | 114 | F | 62 | 964 | 19 |
| E | 120 | M | 61 | 1006 | 23 |
| E | 121 | F | 64 | 1204 | 22 |
| E | 127 | F | 70 | 1684 | 23 |
| E | 128 | F | 62 | 1022 | 18 |
| E | 133 | M | 54 | 506 | 22 |
| E | 135 | M | 53 | 564 | 23 |
| E | 137 | M | 54 | 618 | 27 |
| E | 139 | M | 52 | 552 | 21 |
| E | 141 | M | 55 | 608 | 27 |
| E | 149 | M | 51 | 558 | 25 |
| E | 153 | F | 61 | 1494 | 22 |
| E | 154 | F | 62 | 1294 | 21 |
| E | 161 | F | 57 | 832 | 27 |
| E | 162 | F | 58 | 1054 | 22 |
| E | 218 | F | 55 | 700 | 28 |
| E | 225 | F | 36 | 240 | 9 |
| E | 226 | F | 57 | 878 | 25 |
| E | 245 | F | 70 | 1346 | 24 |
| E | 247 | M | 61 | 960 | 21 |
| E | 249 | F | 74 | 1950 | 27 |
| E | 253 | F | 72 | 1920 | 28 |
| E | 255 | F | 63 | 1170 | 25 |
| E | 258 | M | 63 | 1136 | 25 |
| E | 263 | F | 71 | 2236 | 24 |
| - | 266 | M | 58 | 862 | 20 |
| - | 267 | F | 56 | 724 | 20 |
| - | 268 | M | 60 | 1024 | 20 |

| | | | | | |
|---|-----|---|----|------|----|
| - | 270 | F | 75 | 1251 | 21 |
| - | 271 | F | 65 | 1346 | 28 |
| - | 272 | F | 66 | 1432 | 19 |